

論文 / 著書情報
Article / Book Information

題目(和文)	Finger Angle and Force Estimation using Array EMG system
Title(English)	Finger Angle and Force Estimation using Array EMG system
著者(和文)	STAPORNCHASITS
Author(English)	Sorawit Stapornchaisit
出典(和文)	学位:博士(学術), 学位授与機関:東京工業大学, 報告番号:甲第11664号, 授与年月日:2020年9月25日, 学位の種別:課程博士, 審査員:小池 康晴,金子 寛彦,八木 透,長谷川 晶一,吉村 奈津江
Citation(English)	Degree:Doctor (Academic), Conferring organization: Tokyo Institute of Technology, Report number:甲第11664号, Conferred date:2020/9/25, Degree Type:Course doctor, Examiner:,,,,,
学位種別(和文)	博士論文
Type(English)	Doctoral Thesis

Tokyo Institute of Technology
Interdisciplinary Graduate School of Science and Engineering
Department of Information Processing

**Finger Angle and Force Estimation using
Array EMG system**

Sorawit Stapornchaisit

Submitted in part fulfillment of the requirements for the degree of

Doctor of Philosophy (Ph.D.)

Stapornchaisit Sorawit: *Finger Angle and Force Estimation using Array EMG system*, Doctor of Philosophy (Ph.D), © July 2020

Supervisors:

Professor Koike Yasuharu

Professor Kaneko Hirohiko

Professor Shoichi Hasegawa

Professor Yagi Tohru

Professor Yoshimura Natsue

Location:

Tokyo, Japan

Abstract

Hand and finger provide human with high precision and accuracy for actuator. Those who suffer from hand loss suffer with reduce detailed skill work and need replacement to perform daily task. Fortunately, control command motor of hand and finger reside in forearm and can be measure for prosthetic hand. However, most of the practical work in this field focus on using machine learning and pattern recognition to translate the noisy surface ElectroMyoGraphy (sEMG) signals to pre-defined grip posture without considering physical control of human's hand and finger. The sEMG signal was measure using EMG sensor place on the skin on top of interest muscles which required skill and knowledge of human anatomy. Moreover, the muscles which are able to provide highest quality sEMG signal is limited to 5-7 muscles depend on subject. Those limitation make finger muscles which small and reside deep inside forearm even harder to detect. Here, we present a study using approach from brain signal acquisition using large number of electrode with signal analysis to detect signal from deep under skin. The processed signal was used to estimate finger angle and stiffness by musculoskeletal model to confirm the signal quality and also potential of musculoskeletal model to express finger motion.

Acknowledgements

I would like to express my gratitude to father, mother, sister, and brother who have tirelessly give me support and encouragement throughout the course of my study. This project cannot be done without them.

I would like to show greatest appreciation to my advisor Professor Dr.Koike Yasuharu for his guidance and inspiration. Your idea always amaze me.

I would like to thank Koike lab student and staff members, Dr. Natsue Yoshimura, Dr. Toshihiro Kawase, Dr. Hiyoyuki Kambara, for teach me everything throughout my study.

I am greatly in debt to my professor during the Master's Degree professor, Dr. Chowarit Mitsantisuk, for providing me the chance to pursue my dream.

I am greteful for my friends in Thailand and Australia for their to help me never feel lonely in faraway land.

Finally, I would also like to thank you for your goodness to me, my friend, Thamaruk Patcharavadee for her diligent friendship and energetic advice that help me get though my darkest day.

“The best way to find yourself is to lose yourself in the service of others.”

Dedication

*Dedicated to my family,
and the loving memory of Sunee and Gimhou Stapornchaisit ,
my dear grandmother and grandfather.*

*Your presence we miss,
Your memory we treasure,
Forgetting you never.*

Contents

Abstract	ii
Acknowledgements	iii
1 Introduction	1
1.1 Human hand	2
1.1.1 Natural Hand Control	2
1.1.2 Electromyography (EMG) signal	2
1.2 Mykin muscle model	3
2 Backgrounds and Aims	5
2.1 Human Hand	5
2.1.1 Thumb Finger	6
2.1.2 Other Finger	8
2.2 sEMG signal	12
2.2.1 Biosemi	12

2.2.2	sEMG pre-processing	13
2.2.3	Limitation of EMG signal	17
2.3	Aims	18
3	Finger angle and force estimation using musculoskeletal model	19
3.1	Aim of this section	20
3.2	Methodology	20
3.2.1	Musculoskeletal Model	21
3.2.2	Linear Regression Model	24
3.3	Experiment Setup	25
3.3.1	Experiment Protocol	26
3.3.2	Performance Indicator	27
3.4	Result	29
3.5	Discussion	30
4	Array sEMG system for deep muscles investigation.	34
4.1	Aim of this section	36
4.2	Methodology	36
4.2.1	Subjects	36
4.2.2	Experiment Protocol	37
4.2.3	Independent Component analysis (ICA)	39

4.2.4	Topology plot to investigate spacial data of independent component (IC)	41
4.2.5	Selection of IC data	43
4.2.6	Finger angle tracking using realsense camera with convolutional-pose-machine	46
4.2.7	Data acquisition	50
4.2.8	Finger angle regression model	51
4.2.9	Performance Indicators	51
4.3	Results	51
4.4	Discussion	54
4.5	Conclusions	57
5	Topology plot of multiple subject.	59
5.1	Aim of this section	59
5.2	Topology plot of each subject	59
5.2.1	Thumb finger	60
5.2.2	Index finger	61
5.2.3	Middle finger	62
5.2.4	Ring finger	62
5.2.5	Pinky finger	63
5.2.6	Average Result	64

5.3 Dipole of deep muscles signal	65
6 Conclusion	67
6.1 Summary	67
6.2 Aim result	69
6.3 Future work	70

List of Tables

- 2.1 The relative force applied by each muscles in forearm connect to thumb finger in different thumb motions [14] 9

- 4.1 Summary of average statistic value from 10 subjects of Figure 4.20 and Figure 4.21, foe reference. 55

- 4.2 Array EMG system advantage to conventional EMG sensor . . . 58

List of Figures

1.1	Sample of EMG signal from Trigno Wireless EMG sensor (Left) and it rectified version (right)	3
1.2	Mykin model was arrange in arm position which show mechanical of biceps as gear and spring [30]	4
2.1	Flexor pollicis longus muscle (FPL) [11]	6
2.2	Abductor pollicis longus muscle (APL) [11]	7
2.3	Extensor pollicis longus muscle (EPL) [11]	7
2.4	Extensor pollicis brevis muscle (EPB) [11]	8
2.5	Motions of thumb [25]	8
2.6	Dorsal interossei muscles [11]	9
2.7	Lumbricals muscles [11]	9
2.8	Flexor digitorum superficialis (FDS) [11]	10
2.9	Flexor digitorum profundus (FDP) [11]	10
2.10	Extensor digitorum (ED) [11]	11

2.11 Extensor indicis (EI) [11]	11
2.12 Index finger motions [2]	12
2.13 Bio-semi EEG acquisition system [5]	13
2.14 Head Cap 160 medium size [5].	14
2.15 Lumbricals muscles [5]	14
3.1 Structure of musculoskeletal model [16].	21
3.2 Stimulus was shown by monitor place 2.5 meters away from subjects in motion capture environment.	25
3.3 Trigno Wireless surface EMG sensors were placed on Flexor Pollicis Longus (FPL), Flexor Digitorum Superficialis (FDS), Extensor Pollicis Brevis (EPB), and Extensor Indicis (EI).	26
3.4 The protocol was 3 seconds of activation and 3 seconds of rest between activations. In one trial, in order to ensure the performance of our model to estimate small force, we separated flexion motion into full flexion and half flexion.	27
3.5 We used replicate version of ReachMan robot [40] and designed to separate each side of ReachMan robot to accommodate only thumb and index finger.	28
3.6 The estimate angle was compared with measured finger angles in time serial (Correlation Coefficient: 0.83) Red: Musculoskeletal model (MSM) , Yellow: Linear Regression model (LRM), Blue: Measured from Optitrack.	29

3.7	Thumb finger angle correlation and RMSE between estimated angle using musculoskeletal model, linear regression, and measured angle using Optitrack system.	30
3.8	Index finger angle correlation and RMSE between estimated angle using musculoskeletal model, linear regression, and measured angle using Optitrack system.	31
3.9	The estimate thumb force was compared with measured finger force in time serial (CC is 0.92) with blue line: estimated from MSM or LRM red line: measured from optitrack motion tracking.	32
3.10	Finger force correlation and RMSE between estimated force using musculoskeletal model, linear regression, and measured force using ReachMan Robot.	32
3.11	Finger force correlation and RMSE between estimated force using musculoskeletal model, linear regression, and measured force using ReachMan Robot.	33
4.1	The arm mask was made with each sensor size around 10 millimeter and place apart with distant of minimal 15 millimeter. Pattern of placement was 10 column horizontally and 5 row vertically on both side (100 position).	37
4.2	The arm mask was made with each sensor size around 10 millimeter and place apart with distant of minimal 15 millimeter. Pattern of placement was 10 column horizontally and 5 row vertically on both side (100 position).	38

4.3	Experiment flow for train data and test data, the finger Thumb, Index, Middle, Ring, and Pinky. In flexion, subject flex finger to 0.9 ± 0.175 rad or 162 ± 10 degrees for 2 seconds. rested for 2 seconds, extend finger to -0.20 rad or -36 degree) for 2 seconds, and rested for for 2 seconds.	38
4.4	Example time serial data. Each section of graph show the separation using stimulus signal (trigger).	39
4.5	Configuration (July 2018) of topology plot for show IC weight as color from -1 (blue) to 0 (green) to 1 (red). Identify the source of IC data on the spatial array EMG system. Topology plot find and match the relation between weight of IC and electrode channel.	41
4.6	16 IC with top score CC value.	41
4.7	The general location of muscles activation according to anatomy data according to finger motion (flexion and extension) and finger.	42
4.8	Time serial show the period of flexion and exntension of 32 IC from thumb flexion and extension motion	43
4.9	Topology plot show the location of 32 IC from thumb flexion and extension motion	44
4.10	Identify the different between wrist and finger muscles signal. We check the location of muscles using anatomy data, we found. 2 wrist muscles, 2 finger muscles, and 1 thumb muscles.	45
4.11	We add the sensor number to represent which sensor row should response to that muscles.	46

4.12 IC activation in time serial with indicate griping period and component 1, 5, and 9 which we interested.	47
4.13 IC activation in time serial with indicate griping period and component 27 which we interested.	47
4.14 The topology plot of component 1, 5, 9, and 27.	48
4.15 Topology plot from IC that might indicate deep muscles.	48
4.16 Left: example of data from convolutional-pose-machines. Right: the finger angle was defined as normalized root mean square error (NRMSE) in 2D space.	48
4.17 Example of bio-semi eletrode sensor in first experiment, other experiment also use the same pattern, please notice the CMS and DRL electrodes. The location of this electrodes need to changes according to subject with 1. on the back of hand 4 centimeters apart, 2. between the hand and upper arm, 3. in position A26 and B26.	50
4.18 Example of time serial data of index finger between estimated using MSM and measurement from realsense camera with convolutional-pose-machine.	53
4.19 Research analysis flow.	53
4.20 Performance of proposed method in first analysis: 5 train data for training and 5 test data for testing. The correlative coefficient was in boxplot and root-mean-squre-error in barplot. number of data = 50 (10 subjects * 5 tests).	54

4.21	Performance of proposed method in second analysis: 1 test data for training and 4 test data for testing. 5-fold validation was adapted to ensure non-bias result. The correlative coefficient was in boxplot and root-mean-square-error in barplot. number of data = 50 (10 subjects * 5 tests).	56
5.1	Reference to the name of each location in topology plot.	60
5.2	Topology plot of thumb flexor from 10 subjects participate in previous study.	60
5.3	Topology plot of thumb extensor from 10 subjects participate in previous study.	61
5.4	Topology plot of index flexor from 10 subjects participate in previous study.	61
5.5	Topology plot of index extensor from 10 subjects participate in previous study.	62
5.6	Topology plot of middle flexor from 10 subjects participate in previous study.	62
5.7	Topology plot of middle extensor from 10 subjects participate in previous study.	63
5.8	Topology plot of ring flexor from 10 subjects participate in previous study.	63
5.9	Topology plot of ring extensor from 10 subjects participate in previous study.	63

5.10 Topology plot of pinky flexor from 10 subjects participate in previous study.	64
5.11 Topology plot of pinky extensor from 10 subjects participate in previous study.	64
5.12 Topology plot of average of all subject separate in each finger. . .	65
5.13 Topology plot of component that represent grip and open motion.	65
5.14 Topology plot of component that represent wrist flexion and extension motion.	66

Chapter 1

Introduction

The human hand is one of the human's extremity consists of five fingers to create intricate primary tools that human use to interact with environment. This tools allow us to not only feel the world but also built and controlled other tools make from our understanding of surroundings. However, we might have to lose it before we can understand the power of small but crucial device to our daily life. In year 1996 U.S.A., estimated 1,285,000 persons living with limb lose (excluding finger and toes) with increasing around 50,000 every year. While this happens, thank to rapid advances in engineering and biotechnology, prosthetic hand with high accuracy and force adjustment in finger control can mimic human finger motions. The problem is how to capture human's intention to control finger, surface ElectroMyoGraphy (sEMG) was used in many researches [3, 13, 15, 17, 27, 39] as control signal to provide non physical control for prosthetic hand. Multiple models was proposed to classify hand postures from EMG signals. And some group also succeeded in control finger and wrist with predetermined grips [12]. However, main functionality still depend on switching hand predefined grip postures which limit the number of postures [36].

1.1 Human hand

The human hand is a versatile and miraculous instrument that serves us extremely well in multitude of way with large number of degree of freedom (DoFs). Combine with multi-sensory units that enable us to interact with environment [10]. We successfully use our hands to contact objects and to extract information about them, such as surface texture, compliance, weight, shape, size, orientation, and thermal properties. Human also demonstrate impressive manual dexterity when reaching for, grasping, and subsequently manipulating objects within arm's reach.

1.1.1 Natural Hand Control

Natural limbs are pulled back and stretch

Recent studies by Santello and Soechting [28], show connection between the central nervous system (CNS) that provide coordinates with many muscles when using hand. This also indicate CNS might control more muscles than are minimally required to perform certain task. This phenomenon called redundancy/abundance problem [4]. Due to redundancy of muscles, this problem leads to an infinite number of solutions for similar tasks and in the case of prehensile actions, elemental variables can be associated with forces and moments of force produced by individual fingers. Meanwhile, performance variable may be associated with the total force and moment of force applied to the hand-held object.

1.1.2 Electromyography (EMG) signal

Electromyography (EMG) generated by muscle cells when neuron signal was receive which generate electric potential activity as shown in Figure 1.1. The

signals was used to detect medical abnormalities, activation level, recruitment order, and analyze the bio-mechanics of human or animal movement. Conventionally, EMG is recorded using a device called an electromyograph and write the voltage directly to paper called electromyogram [7].

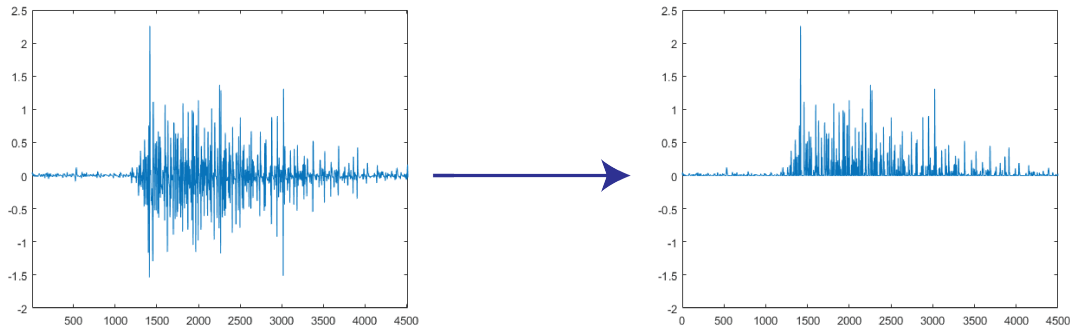


Figure 1.1: Sample of EMG signal from Trigno Wireless EMG sensor (Left) and its rectified version (right)

The electric potential is generated when a motor neuron signal from spinal cord arrives at the muscles's motor end plate which causes a release of Calcium ions (Ca^{2+}) that consequently generate ion exchanges across the muscles membrane [7]. The more muscles that activate, the greater amplitude of action potential and the greater the EMG reading.

1.2 Mykin muscle model

Mykim model designed from human arm in horizontal plane with two muscles manipulator consist of six monoarticular muscles and two biarticular muscles. The mechanical of the bicep is shown as rack-and-pinion gear and a spring connected in series as shown in Figure 1.2 [30].

The Kelvin-Voigt model was used with elastic element for static isometric contraction [23]. Muscle tension T is determined from muscle stiffness $k(u)$ and the stretch length of a muscles $[l_r(u) - l(\theta)]$ as follows

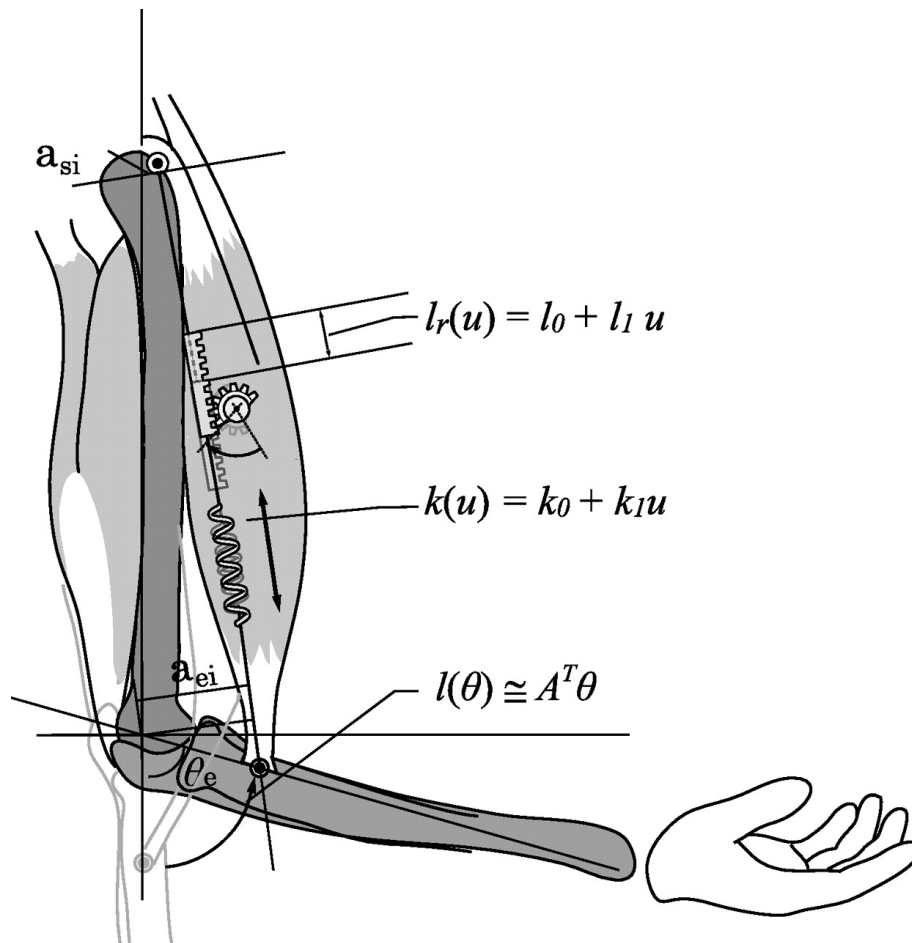


Figure 1.2: Mykin model was arranged in arm position which shows the mechanical of biceps as gear and spring [30]

Chapter 2

Backgrounds and Aims

This chapter will provide the detail about previous work and assumption that used in this thesis. We will talk about human hand, sEMG signal, ICA, Motion capture, and Aim of our research.

2.1 Human Hand

Human hand has 27 degree of freedom (DOF): each finger have 4 consist of 3 for extension and flexion and 1 for abduction and adduction; the thumb is more complicated and has 5 degree of freedom (DOF), leaving 6 degree of freedom (DOF) for the rotation and translation of the wrist. In order to accurately model the hand, a complete structure of muscles, tendons, bones is necessary. The models we used is simplified version following assumptions: 1. The thumb is independent of the other fingers. 2. Adduction and abduction of the finger joint are independent. 3. Motion frequency does not affect joint interdependence [9].

In this research, we focus on 5 finger (thumb, index, middle, ring, pinky) and

due to the muscles location we only considering flexion/extension (1 DOF) for each finger.

2.1.1 Thumb Finger

Muscles connect to thumb finger can be compared with multiple wires that supporting flag poles, the tension force from each muscles help maintain stability in the articulated column formed by the bones of the thumb. Therefore, during thumb motions all muscles attached to thumb are active.

Muscles

The muscles that locate in an extrinsic (forearm) area and attached to thumb are shown below.

1. Flexor pollicis longus muscle (FPL) shown in Figure 2.1,

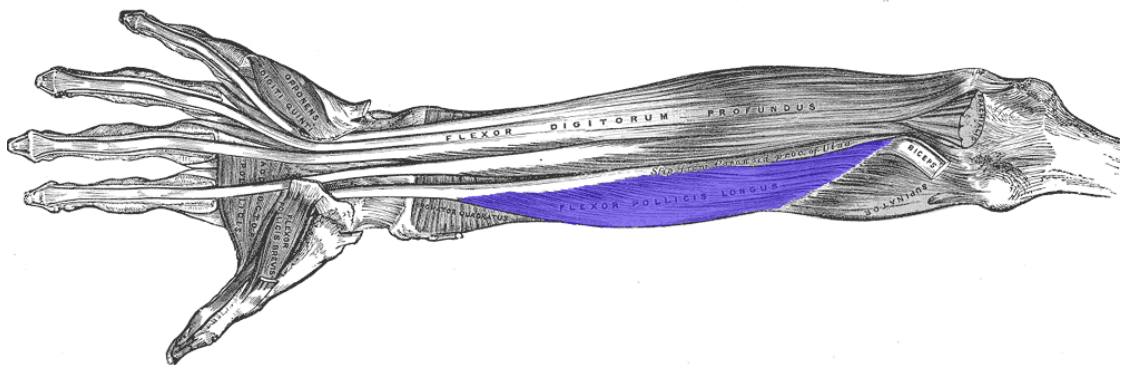


Figure 2.1: Flexor pollicis longus muscle (FPL) [11]

2. Abductor pollicis longus muscle (APL) shown in Figure 2.2.
3. Extensor pollicis longus muscle (EPL) shown in Figure 2.3.
4. Extensor pollicis brevis muscle (EPB) shown in Figure 2.4.

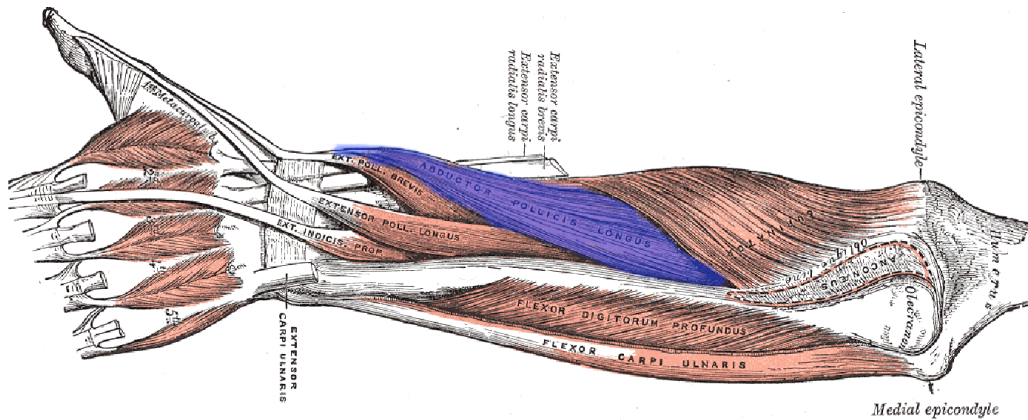


Figure 2.2: Abductor pollicis longus muscle (APL) [11]

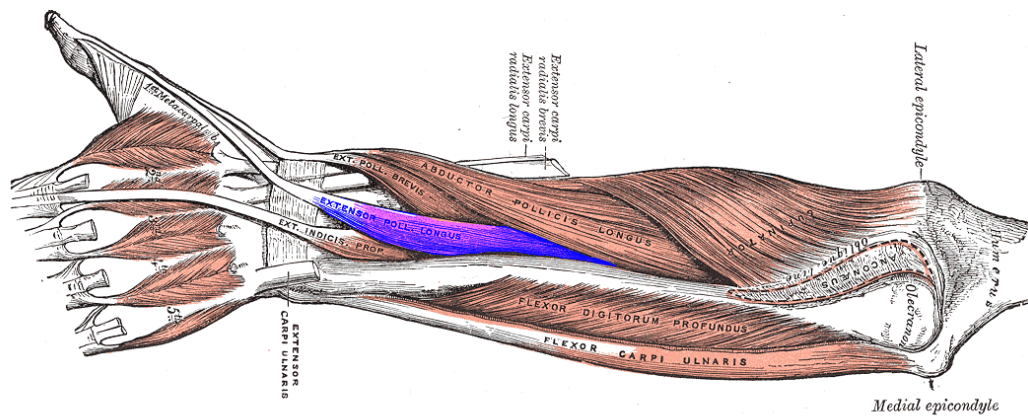


Figure 2.3: Extensor pollicis longus muscle (EPL) [11]

Motions

The motions of thumb also classify into flexion, extension, abduction, adduction, opposition, and reposition as shown in Figure 2.5. The relationship between muscles and finger motions are presented in Table 2.1 The grip motions is combination of flexion and adduction, which is not fully obtainable from forearm muscles. However, the flexion can represent the motions of grip while counter action of extension also obtainable in forearm muscles. Therefore in this research, we focus on obtain flexion and extension motions from Flexor pollicis longus, Extensor pollicis longus, and Extensor pollicis brevis for thumb finger.

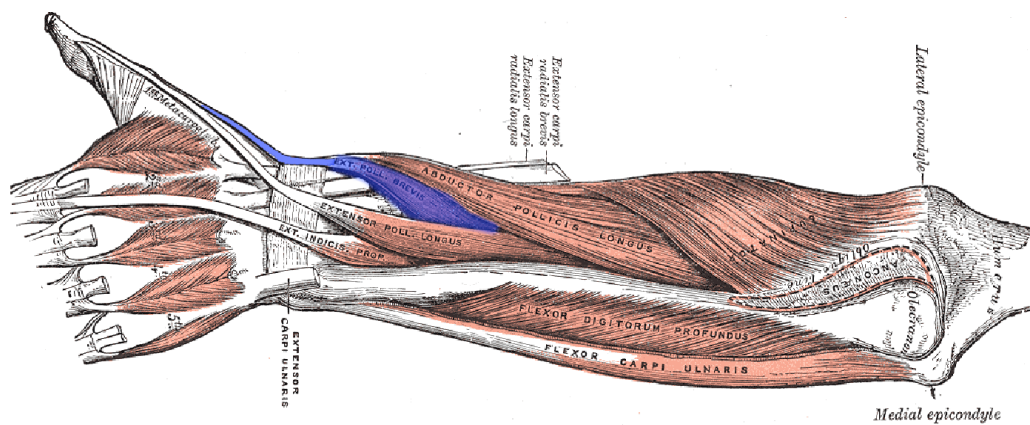


Figure 2.4: Extensor pollicis brevis muscle (EPB) [11]

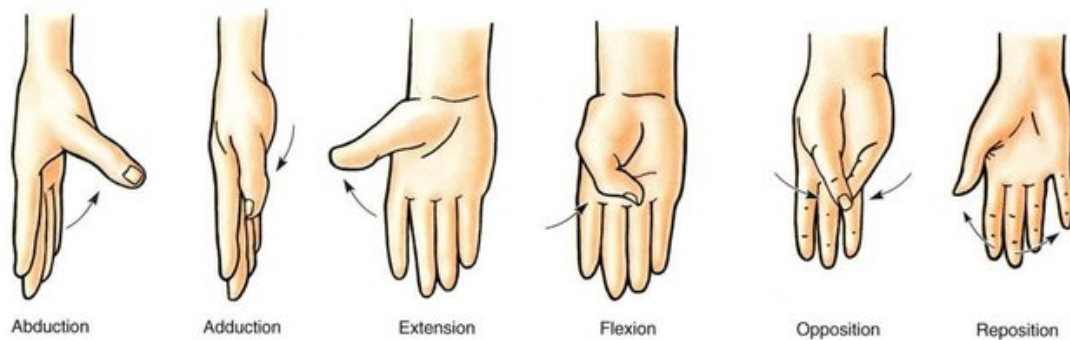


Figure 2.5: Motions of thumb [25]

2.1.2 Other Finger

The muscles of other fingers consist of 6 muscles to stabilize and control the movement of index finger. Pinky finger have one more muscle to perform opposition and reposition attached to it.

Muscles

Two muscles located in hand are interossei in figure 2.6, and lumbrical in figure 2.7 responsible for abduction and adduction movement, also stability but do not contribute to flexion and extension movement.

Four muscles located in extrinsic (forearm) provide flexion and extension move-

	Flexion	Extension	Abduction	Adduction	Opposition	Reposition
Flexor pollicis longus	strong				medium	
Abductor pollicis longus		weak	strong			weak
Extensor pollicis longus		medium	weak			weak
Extensor pollicis brevis		medium	weak			weak

Table 2.1: The relative force applied by each muscles in forearm connect to thumb finger in different thumb motions [14]

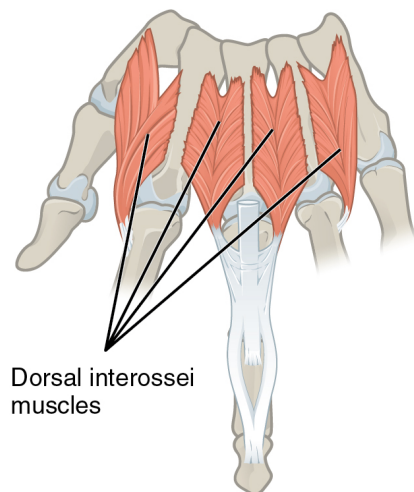


Figure 2.6: Dorsal interossei muscles [11]

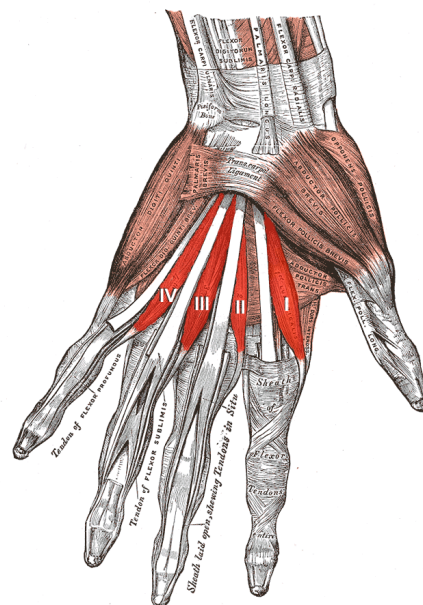


Figure 2.7: Lumbricals muscles [11]

ment consist of the following muscles.

1. Flexor digitorum superficialis (FDS) muscle shown in Figure 2.8 function as flexion of the middle phalanges of the index fingers at the proximal interphalangeal joints. However, under continued contraction, it also flexes the metacarpophalangeal joints and wrist joint.

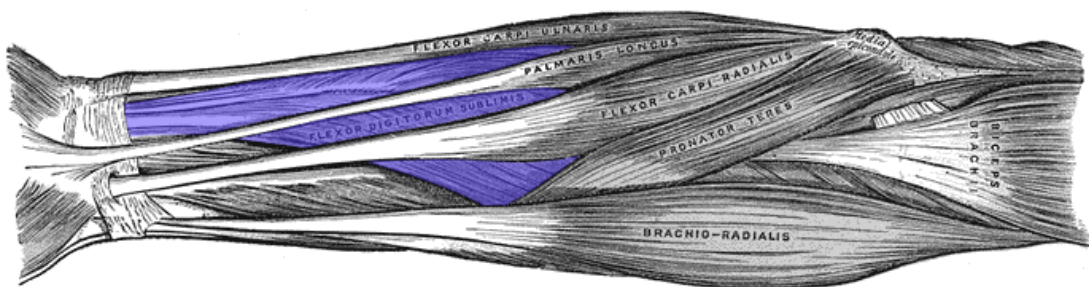


Figure 2.8: Flexor digitorum superficialis (FDS) [11]

2. Flexor digitorum profundus (FDP) muscle shown in Figure 2.9 function as flexor of the wrist, metacarpophalangeal and interphalangeal joints. This muscles support the motions of lumbrical muscles and make the finger cannot fully perform extension if the wrist is fully flexed.

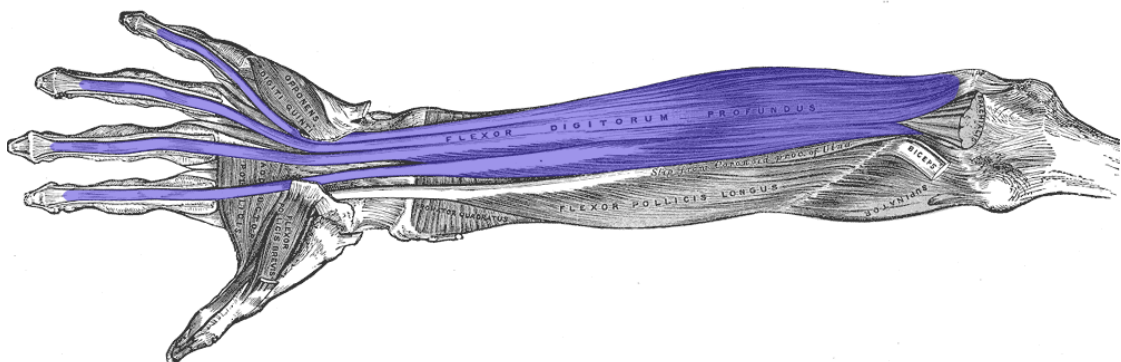


Figure 2.9: Flexor digitorum profundus (FDP) [11]

3. Extensor digitorum (ED) muscle shown in Figure 2.10 function on the

proximal phalanges, acting to extend the metacarpophalangeal joint. Extension of the proximal and distal interphalangeal joints.

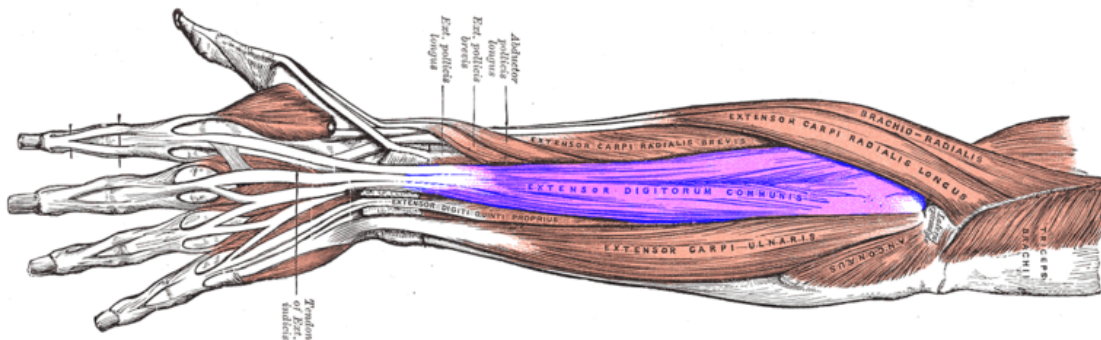


Figure 2.10: Extensor digitorum (ED) [11]

4. Extensor indicis (EI) muscle shown in Figure 2.11 function as extensor of the index finger.

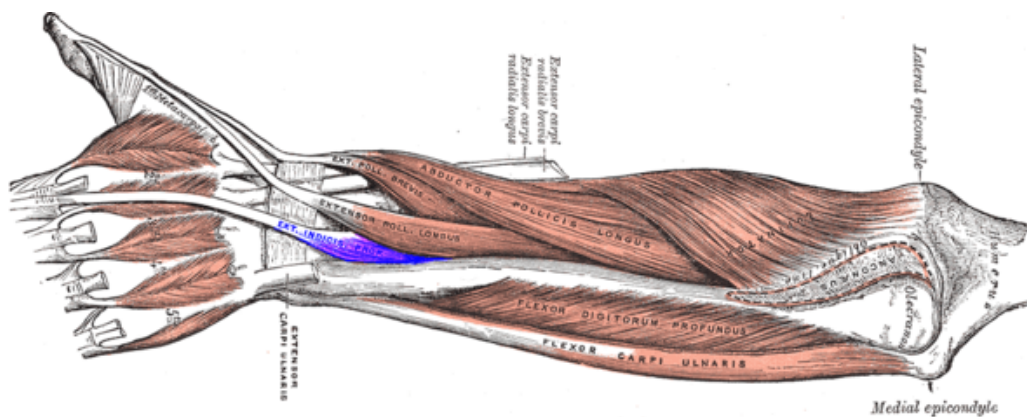


Figure 2.11: Extensor indicis (EI) [11]

Motions

All the motion of other fingers that control by muscles in extrinsic are flexion and extension motions. Therefore, using the same method with thumb finger, we will focus on flexion and extension from flexor digitorum profundus muscles (FDP) and extensor indicis (EI) muscles of the index finger.

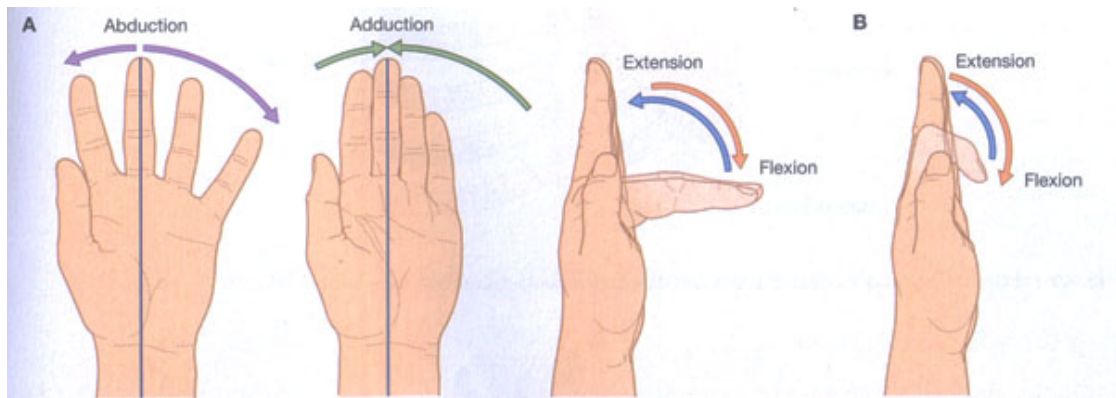


Figure 2.12: Index finger motions [2]

2.2 sEMG signal

EMG signal used in this thesis are monopole EMG signal using Bio-semi EEG system. Original desired to collect EEG data from brain but we convert it to use with EMG signal from forearm. We also include conventional sEMG processing method in this section.

2.2.1 Biosemi

Bio-semi is the new standards for multi channel, high resolution biopotential measurement system for research applications. The system can increase the number of electrode to 256+8 electrode and 7 sensor channels in a single ultra compact box as shown in Figure 2.13

Conventional Bio-semi system used head cap with electrode holder for EEG acquisition system as shown in Figure 2.14. The layout of each electrodes are shown in Figure 2.15.

Head cap save time in the acquisition process of multi-channel EEG. All EEG caps will have electrodes which are placed according to international standards. EEG headsets should come with a variety of sizing options and be easily ad-



Figure 2.13: Bio-semi EEG acquisition system [5]

justed to fit subject anatomy.

2.2.2 sEMG pre-processing

Motor units are skeletal muscles which are form of striated muscle tissue that is under the voluntary control of the somatic nervous system. As the number of activated motor unit increase mean amplitude of EMG signal was increase as well. Therefore, the maximum amplitude of EMG measured in an experiment can indicate amplitude of action force of muscles.

The electrochemical signals will arrive at neuromuscular junction which is the gap between motor neuron and muscles fiber that use chemical to communicate. Muscles contraction start and result in the depolarization of the muscle



Figure 2.14: Head Cap 160 medium size [5]

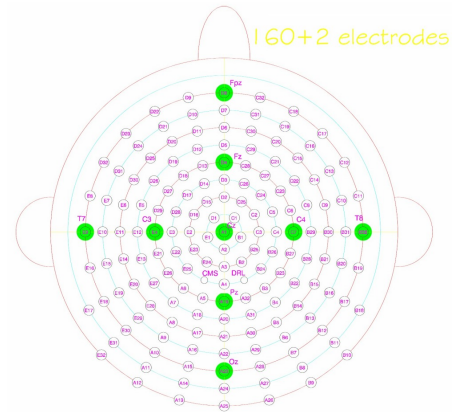


Figure 2.15: Lumbricals muscles [5]

fiber, which is propagated by saltatory conduction (propagation of action potentials along myelinated axons from one node of Ranvier to the next node, increasing the conduction velocity of action potentials long its axon. While Ca ion release in motor units, the muscles contraction will continue active and result in slowly declined active contraction due to the Sarco/endoplasmic reticulum calcium-ATPase (SERCA) pumps calcium ion back. Result in Ca ion declines to resting levels, the force declines and relaxation occurs.

The processing step of EMG signal from bio-semi system can be classified roughly into 5 steps of Re-referencing, Rectification, low-pass filter, and Normalization.

Re-referencing

The bio-semi have active electrode, therefore it can record data reference-free and use re-reference after experiment. The re-reference using average reference from all channel [5].

Re-referencing was used with average re-reference in EEGLAB plugin on MATLAB 2019b platform. The method was calculate average value of all electrode and use that value as nominal signal for all electrode. This method proof to be effective in conventional EEG signal pre-processing.

Rectification

Rectification translate raw EMG signal to all positive. The propose of rectification the signal was to ensure the raw signal does not provide average zero, this was affect of raw WMG signal have both positive and negative value. There is mainly two method to rectify EMG signal.

Absolute filter inverse all negative signal into positive signal and provide good muscles activation graph which increase stability of EMG signal. However, reference electrode should be firmly place on skin that provide minimal distant to bone to reduce noise as much as possible. Another method is to use multiple electrode in the same area and average the reference signal across all electrode. Fail to provide good reference signal will lead to abnormal high muscles activity that got enhance by absolute rectification method.

Positive filter rejects all negative signal and leaves only positive signal as shown in Figure 1.1, the filter might reject some actual muscles activity but also reduce noise from reference. Best application for the positive filter is the muscles that provide very high EMG signal and movement noise. However, moving artifact and motions noise still affect the amplitude and quality of EMG signal.

Other methods also include EMG signal decomposition. This used theory that EMG signals measure by surface electrode made up of several motor units under that electrode area.

Normalization

Different person has a different characteristic of muscles, the same activation potential of the EMG signal will not produce same force or muscles activity. Moreover after extended exercise or muscles recovery period, the relation between force, EMG signal, and joint angle can be changes. Therefore, the method

to simplify EMG signal from different people that produce different force for different joint angle called normalization. There are four methods considered in this thesis,

- Maximum (peak) activation levels during maximum contractions, the most common method to normalize EMG signals from muscles of interest recorded from the same muscles during a maximal voluntary isometric contraction (MVIC) as a reference value. This method required reference test before every experiment by measure the muscles of interest and ask subject to produce the maximum force on force sensor. Based on the repeat-ability between tests subjects, many research recommend to conduct MVIC 3 times and provide rest time between each experiment at least 2 minutes to avoid fatigue [22].

After normalization, EMG signal is considering as the percentile of reference EMG signal with force and lead to easy force estimation from muscles by EMG signal. However, this reference is based on isometric contraction which means the joint angle must remain the same as the length of muscles must not changes.

- Peak or mean activation levels obtained during the task under investing, this method based on the maximum value given by subject throughout the experiment and produce high reliability between experiments. However, the use of this method to normalize EMG data to compare muscles activation levels between individuals and between different muscles in the experiment is not valid. The reason is the reference value is in task and changes according to subject, it cannot compare muscle activation levels between different tasks [1, 38, 6, 18].
- Activation levels during sub-maximal isometric contractions, the main

problem of the first and second method is the difficulty in getting subjects to mobilize their maximal potential especially in symptomatic subjects who cannot perform a maximum contraction because of pain, muscles inhibition, or risk of injury [6, 18, 35]. Therefore, the use of submaximal contraction levels produces reference EMG levels for the purposes of normalizing the EMG signal by use EMGs from contractions that lower than 80% of maximal voluntary isometric contraction (MVIC) [8].

In summary, only MVICs method can be validly used to compare muscle activity levels and patterns between muscles, tasks, and individuals but the subject are constant to isometric contraction and over maximum value are possible. Peak or mean activation levels obtained during the task under investing also possible because the musculoskeletal model also required individual parameters.

2.2.3 Limitation of EMG signal

Surface EMG signal have limited usage due to problems associated with it. As the muscles activity voltage travels to the surface of the skin, the Adipose tissue (fat) can affect EMG recordings by obstructing the voltage.

EMG signal are typically accurate with individuals with lower body fat and complaint skin. For example, young people is more accurate than old. Also the cross talk between muscles reduce reliability of the signal. Deep muscles also hard to detect.

2.3 Aims

In this study, we will be considering the best method to detect EMG signal from deep muscles (finger muscles) by comparing between conventional method and new EMG array method. Therefore, three objectives we would like to achieve from this study is;

1. The possibility to change from conventional pattern recognition system to regression which is the same as musculoskeletal model.
2. The method to provide better deep muscles EMG signal by signal processing many sensors around forearm.
3. The performance of such method compared with conventional one.

Chapter 3

Finger angle and force estimation using musculoskeletal model

Conventional prosthetic hand control system controls finger using pattern recognition from surface ElectroMyoGraphy signal (EMG) from muscles in the forearm. Most of the finger muscles are located in the forearm with tendon connected to the finger, elbow, shoulder skeletal. Pattern recognition can provide only limited posture and grip motion which is different from natural musculoskeletal models of hand. Although science understands the relation between muscle activity and finger motion but most prosthetic arms still operate using the conventional method of pattern recognition such as machine learning and artificial neuron network.

The proposed method used sEMG from muscles and movement of finger to train model to estimate equilibrium position and stiffness in one degree of freedom (DOF) for each finger call musculoskeletal model. In this study, we interested in using the same principle of the musculoskeletal model to estimate equilibrium position and stiffness of thumb and index finger separately by mea-

suring position in 3-dimensional space. The result will be confirmed by measuring position, force and EMG of the subject simultaneously.

3.1 Aim of this section

This study provided new study in the field of thumb and index finger angle and force estimation. The main target is to measure the characteristic of thumb and index finger muscles using proposed MSM. The sEMG was considered as muscle contractions and motion of thumb and index finger was simplified into flexion (+) and extension (-) motions.

3.2 Methodology

The method used to calculate thumb and index finger angle from surface EMG signal is mathematic equation derived from MSM. Stiffness and force command were converted into torque using simple spring theory, then applied to motor.

All calculations were performed in computer with specification of;

1. Microsoft Windows 10 64 bit
2. Processor Intel(R) Xeon(R) CPU E5-1680 v4 @ 3.40GHz, 3401 Mhz, 8 Core(s), 16 Logical Processor(s)
3. Installed Physical Memory (RAM) 64.0 GB
4. Intel(R) C610 series/X99 chipset
5. NVIDIA Quadro P2000

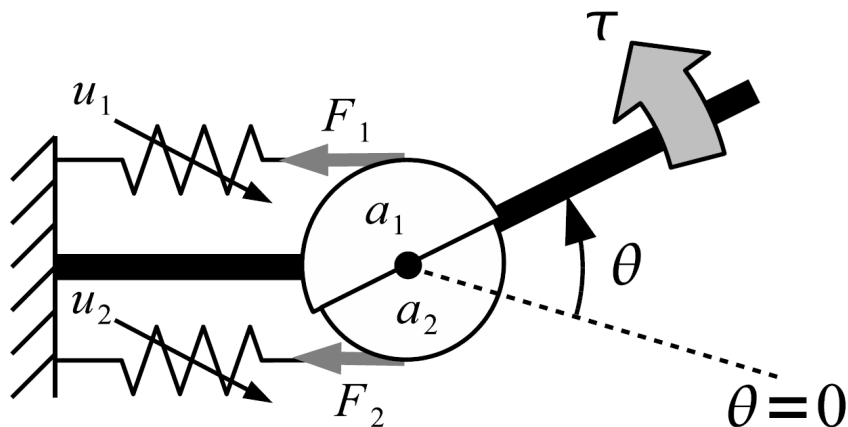


Figure 3.1: Structure of musculoskeletal model [16].

3.2.1 Musculoskeletal Model

The musculoskeletal model (MSM) is second order linear regression with constrain on some parameters to reduce the complexity of finger musculoskeletal structure according to Mykin model [40]. The model using 2 muscles as springs connect to one degree of freedom joint and controlled by muscle activation as shown in Figure 3.1. In real anatomy, musculoskeletal structure is consist of more than single muscles for joint and multiple supported muscles for stabilization. However, most of them work as an independent group that provide almost uniform motions for finger motion [30]. In this paper, flexor muscles was referred as muscle 1 and extensor muscles was referred as muscle 2.

According to Wondaie R. et al, the location of sEMG sensor was identified with anatomy and motion of subject according to human forearm [26]. Thus, our research started from select the interested muscles that responsible for finger motion. In this case, flexion and extension motion. Also the muscles need to be large enough to acquired good sEMG signal. Thumb has 4 muscles connected, and finger have 5 muscles. For this study, we select:

For thumb finger;

1. Flexor pollicis longus muscles (FPL)
2. Extensor pollicis brevis muscle (EPB)

For index finger;

1. Flexor digitorum superficialis (FDS)
2. Extensor digitorum (ED)

The sEMG sensor was placed by measuring sEMG signal while asking the subject to move the finger in flexion and extension motions to find the signal. The position also received small adjustments multiple times. Finally, the reasonable signal-to-noise ratio of the subject was acquired. In case of signal strength reduction, the data of that particular experiment was rejected and the subject repeated the experiment.

Muscles Tension

The muscle tension or force was calculated from muscle activity in which referred by sEMG signal of muscles i when i represent flexion muscle and extension muscle as 1 and 2, respectively. The sEMG signal was rectified, noise level rejected and normalized with filters of the following low-pass filters with impulse response characteristics shown in Equation 3.1. The characteristics were derived from the study on estimation of joint torque with neural networks which reproduce latent, contraction and relaxation period between sEMG signal and muscle tension [21].

$$h(t) = 6.44 \times (e^{-10.80t} - e^{-16.52t}) \quad (3.1)$$

The tension F_i of muscles i is expressed as Equation 3.2.

$$F_i = (k_{0i} + k_{1i}u_i)(l_{0i} + l_{1i}u_i - a_i\theta) \quad (3.2)$$

a_i denotes moment arm of muscle i ; k_{0i} , k_{1i} , l_{0i} , l_{1i} , parameters (all in positive values) to define the characteristics of muscle i , θ indicate the joint angles, where angle in flexion is expressed as positive. Signs for moment arm are expressed as follows to indicate the effects resulting from the difference in position of the muscles: $a_1 > 0$, $a_2 < 0$.

Joint Torque, Equilibrium Points and Stiffness

The torque of each muscle represented by muscle contraction, string constant, and length of muscles, which were separated between flexor and extensor. The torque of said joint was expressed by adding up torque of flexor and extensor as shown in Equation 3.3 [27], where torque in the flexion direction was expressed as the positive value.

$$\tau = \sum_{i=1}^2 a_i(k_{0i} + k_{1i}u_i)(l_{0i} + l_{1i}u_i - a_i\theta) \quad (3.3)$$

Equilibrium point of the joint was calculated by solving Equation 3.3 for the joint angle (θ) that $\tau = 0$. Equilibrium points were defined as the angles at which torque generated by muscles was balanced to stop when no external forces were applied to the joints as shown in Equation 3.4 [27].

$$\Theta_{eq} = \frac{\sum_{i=1}^2 a_i(k_{0i} + k_{1i}u_i)(l_{0i} + l_{1i}u_i)}{\sum_{i=1}^2 (a_i)^2(k_{0i} + k_{1i}u_i)} \quad (3.4)$$

Stiffness K was defined by torque generated by displacement between equilibrium point and joint angles or partially differentiating Equation 3.3 by joint angles (τ) as shown in Equation 3.5.

$$K = -\frac{\partial \tau}{\partial \theta} = \sum_{i=1}^2 (a_i)^2(k_{0i} + k_{1i}u_i) \quad (3.5)$$

Therefore, the simple spring equation could represent the relations between joint torque, equilibrium point, and stiffness K as show in Equation 3.6.

$$\tau = -K(\theta - \Theta_{eq}) \quad (3.6)$$

3.2.2 Linear Regression Model

Linear Regression Model (LRM) was used in this research to make it easier to understand the impact of MSM and compare it with other conventional models.

$$\theta_{f,i}^l = \beta_{i,0} + \beta_{i,1} * u_{i,1} + \beta_{i,2} * u_{i,2} + \epsilon \quad (3.7)$$

3.3 Experiment Setup

The experiment performed on 10 right-handed male subjects age between 21-28 years old with an average age at 25.2. Subjects were given a command by stimulus program showing the preferred action on the screen which was 2.5 meters away as shown in Figure 3.2. The motion of fingers were captured by Optitrack with Baseline Upper Body + Fingers (33). The markers were placed on proximal interphalangeal joints of thumb finger, distal interphalangeal joints of the index finger, and proximal interphalangeal joints of index finger according to human anatomy.



Figure 3.2: Stimulus was shown by monitor place 2.5 meters away from subjects in motion capture environment.

Surface EMG sensors with local reference were placed on Flexor Pollicis Longus (FPL), Flexor Digitorum Superficialis (FDS), Extensor Pollicis Brevis (EPB), and Extensor Indicis (EI) as shown in Figure 3.3. The wireless EMG sensor and optical motion capture were used to ensure maximum freedom of motion while measuring finger angle and EMG signal, simultaneously. The data from both

devices were synchronized and stored using LSL (lab streaming layer). Each subject performed at least 10 trials with 5 trials for variable estimation and 5 trials for verification choosing randomly. In each trial, the calibration period was set at the start of the trial to reduce noise.

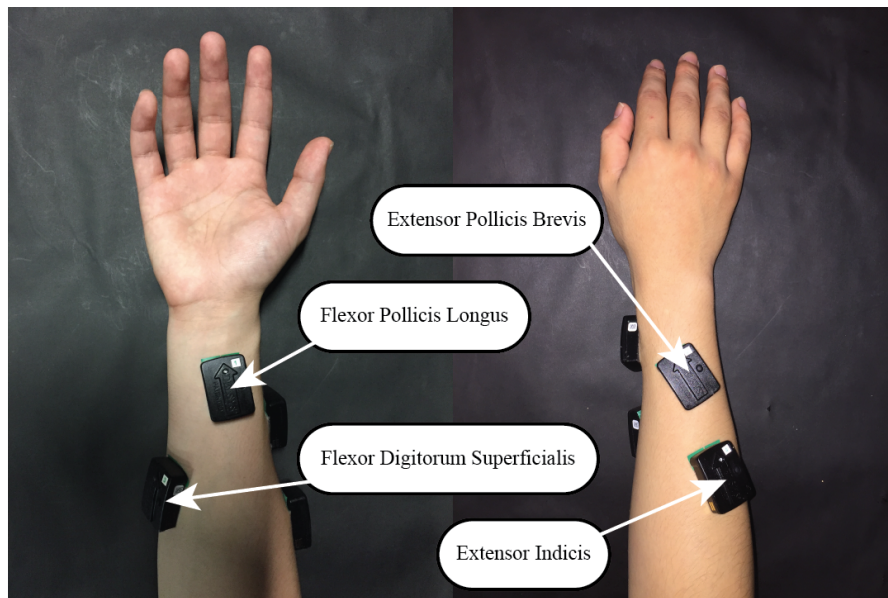


Figure 3.3: Trigno Wireless surface EMG sensors were placed on Flexor Pollicis Longus (FPL), Flexor Digitorum Superficialis (FDS), Extensor Pollicis Brevis (EPB), and Extensor Indicis (EI).

3.3.1 Experiment Protocol

In this study, we used MSM and LRM to estimate finger angle and force from EMG signal. However, due to technical limitation we could not measure both finger angle and force at the same time, resulting in separation of the experiment into two parts of finger angle experiment and finger force experiment.

Finger angle experiment

In order to confirm the performance of MSM on finger, we designed the experiment protocol to measure finger muscle activity and finger motion, simultaneously. The motion we were interested in this research was thumb flexion, thumb

extension, index flexion, and index extension. Previous research provided experiment protocol which able to avoid muscle fatigue [27]. The protocol was 3 seconds of activation and 3 seconds of rest between activations. In one trial, in order to ensure the performance of our model to estimate small force, we separated flexion motion into full flexion and half flexion as shown in Figure 3.4.

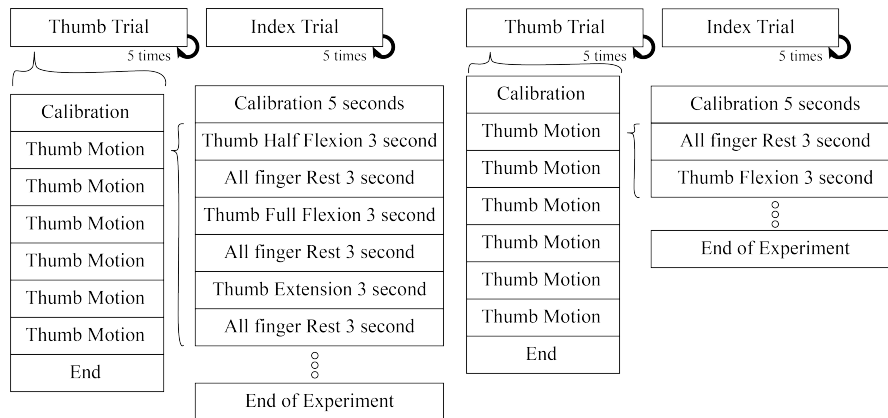


Figure 3.4: The protocol was 3 seconds of activation and 3 seconds of rest between activations. In one trial, in order to ensure the performance of our model to estimate small force, we separated flexion motion into full flexion and half flexion.

Finger force experiment

In order to measure the force from finger, we used replicate version of ReachMan robot [34] and designed to separate each side of ReachMan robot to accommodate only thumb and index finger as shown in Figure 3.5. The experiment protocol was similar to previous finger angle experiment but reduce number of trails to 3 trials per finger to reduce fatigue.

3.3.2 Performance Indicator

We present the result from this study using performance indicators for each subject. correlation coefficient (CC) and Root-mean-square-error (RMSE) was selected.

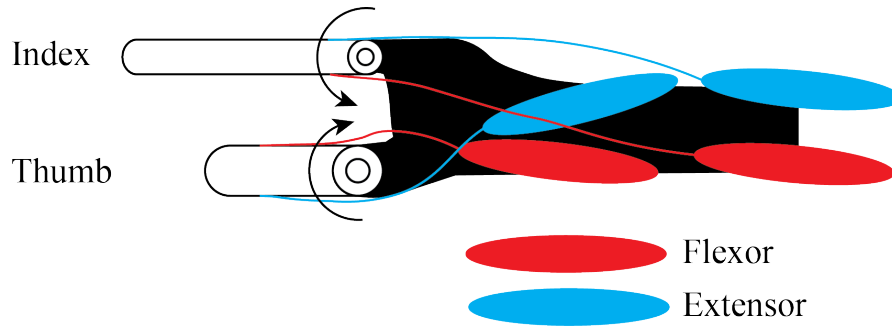


Figure 3.5: We used replicate version of ReachMan robot [40] and designed to separate each side of ReachMan robot to accommodate only thumb and index finger.

Correlation Coefficient

The correlation coefficient (CC) is a method to measure the strength of relationship between two variables. CC range is between -1.0 which represent perfect negative correlation (inverse) and 1.0 represents a perfect positive correlation (increase and decrease the same amount). CC of 0.0 no relationship between two variables. In this study we used equation for correlation coefficient as Equation 3.8.

$$CC = \frac{1}{n-1} \sum_{i=1}^n \left(\frac{x_i - \bar{x}}{S_x} \right) \left(\frac{y_i - \bar{y}}{S_y} \right) \quad (3.8)$$

Root-mean-square-error

The Root-mean-square-error (RMSE) used to measure different of 2 variables. The equation was shown in Equation 3.9.

$$RMSE = \sqrt{\frac{\sum_{i=1}^n (x_i - y_i)^2}{n}} \quad (3.9)$$

3.4 Result

The result in this study was the statistical analysis (CC and RMSE) between measured finger angle, force and estimated finger angle, force from MSM and LRM. Each subject performed 5 trials of each experiment (thumb and index finger). The first trial was used to estimate finger parameter (k_{0i} , k_{1i} , l_{0i} , l_{1i}). And the other 4 trials were used as test, 5-fold verification was performed to generate 20 data of CC and RMSE to ensure the performance of model.

In the first experiment, the estimated angles from MSM and LRM were compared with measured finger angles in time serial as shown in Figure 3.6. The statistical analysis (CC and RMSE) of each subject were shown using box-and-whisker in comparison between MSM and LRM model in Figure 3.7 (thumb finger) and Figure 3.8 (index finger). The result showed different between MSM and LRM average correlation coefficient of 0.05 with RMSE average at 16.12 degree. LRM showed lower CC and higher RMSE which was expected due to lower order of regression.

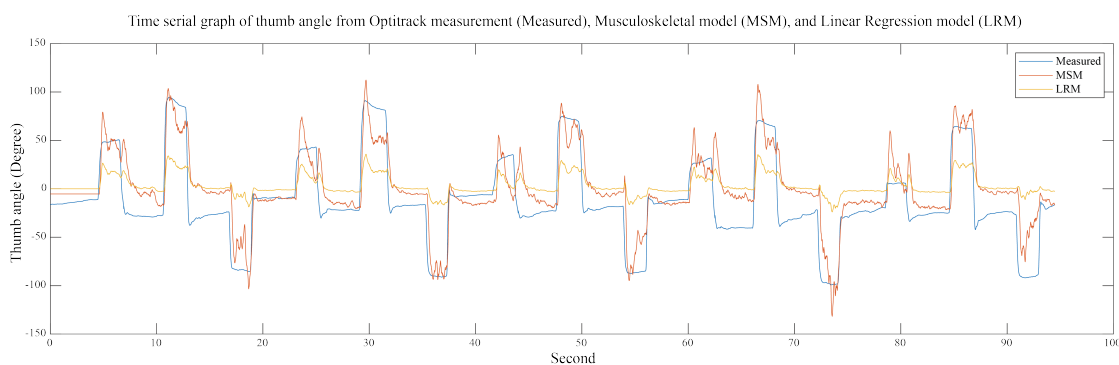


Figure 3.6: The estimate angle was compared with measured finger angles in time serial (Correlation Coefficient: 0.83) Red: Musculoskeletal model (MSM), Yellow: Linear Regression model (LRM), Blue: Measured from Optitrack.

For the second experiment, the estimated force from MSM and LRM were compared with measured finger force in time serial as shown in Figure 3.9. The

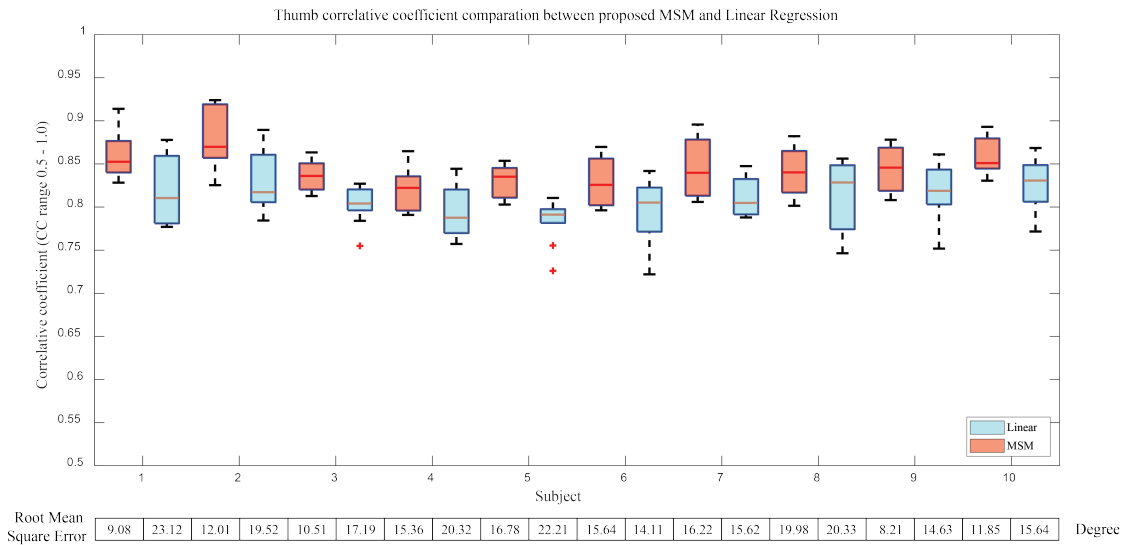


Figure 3.7: Thumb finger angle correlation and RMSE between estimated angle using musculoskeletal model, linear regression, and measured angle using Optitrack system.

statistical analysis (CC and RMSE) of each subject were shown using box-and-whisker in comparison between MSM and LRM model in Figure 3.10 (thumb finger) and Figure 3.11 (index finger).

The p-value of CC values between MSM and LRM calculated by using pair t-test for finger angle were below 0.05 which were considered statistically significant. However, for force estimation, p-value were higher than 0.05 which means no significant difference between MSM and LRM.

3.5 Discussion

Generally, the statistical analysis showed high correlation between sEMG signal and thumb, index angle estimated by MSM and LRM. MSM showed better performance due to 2-order regression. However, MSM was still unable to maintain finger angle during smaller activation after motion due to its lack of damper element.

For the first experiment, the result showed highly consistence CC with differ-

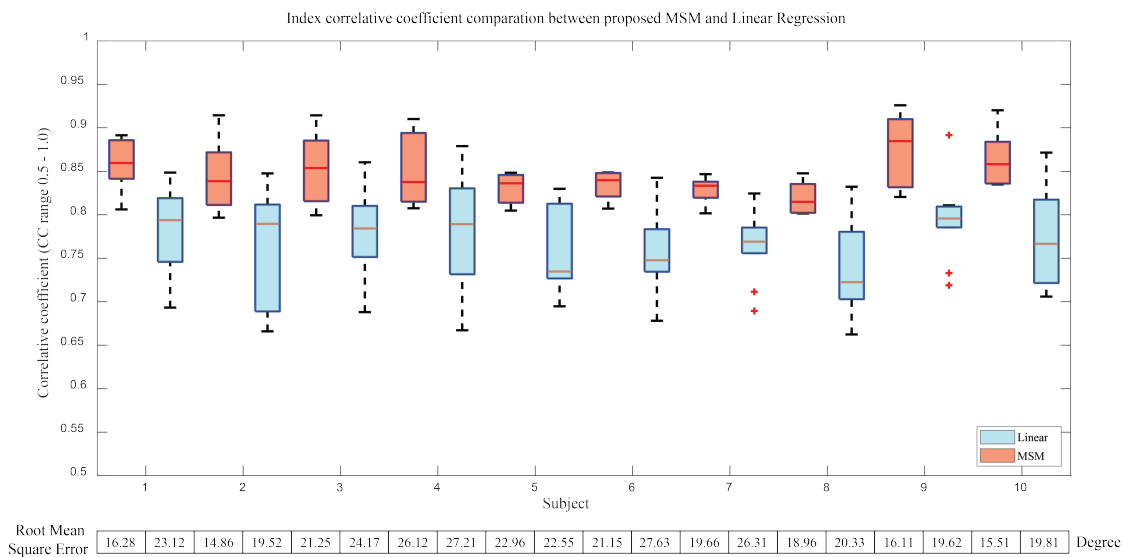


Figure 3.8: Index finger angle correlation and RMSE between estimated angle using musculoskeletal model, linear regression, and measured angle using Optitrack system.

ent around 0.04 ± 0.06 for thumb finger and 0.08 ± 0.06 for index finger which was relatively low in term of CC value. This indicated that MSM and LRM performed very similarly with small improvement. In term of RMSE, it showed similar improvement in the same trend as CC value. Some subject such as subject 8 and 10 showed very small improvement in both CC and RMSE. This indicated the relation between sEMG and finger angle of those subjects to be almost first-order linear. The average RMSE of finger angle was 20 degree which was around 10% (range is 180 degree), This error came from sEMG signal reduction after the target position was reached.

For the second experiment, the result were still consistence for thumb finger but less consistence in index finger. In some subject, the force estimated using LRM showed better performance. The different between MSM and LRM also became much smaller, indicated that finger force might be able to represent using only 1-order linear regression. MSM also showed deep dip before force activation. This happened because subject unconsciously extended their fingers before the experiment which could be reduced by repeating the experiment multiple times

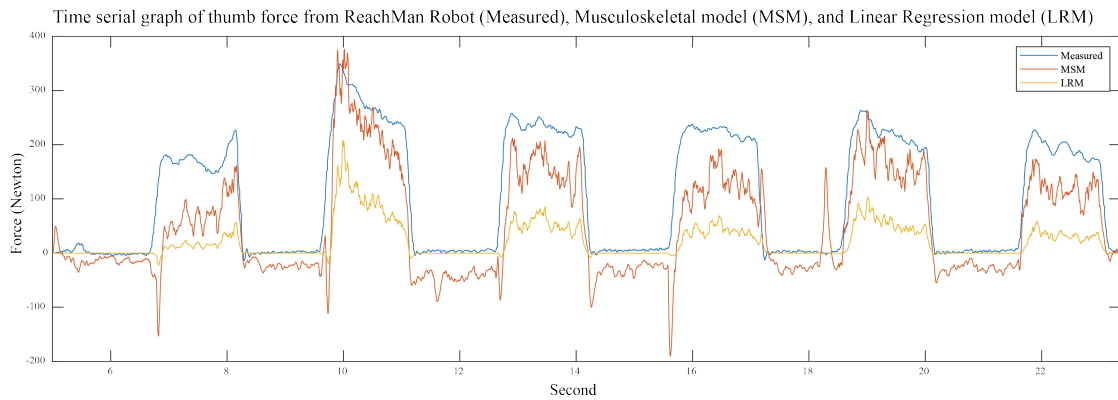


Figure 3.9: The estimate thumb force was compared with measured finger force in time serial (CC is 0.92) with blue line: estimated from MSM or LRM red line: measured from optitrack motion tracking.

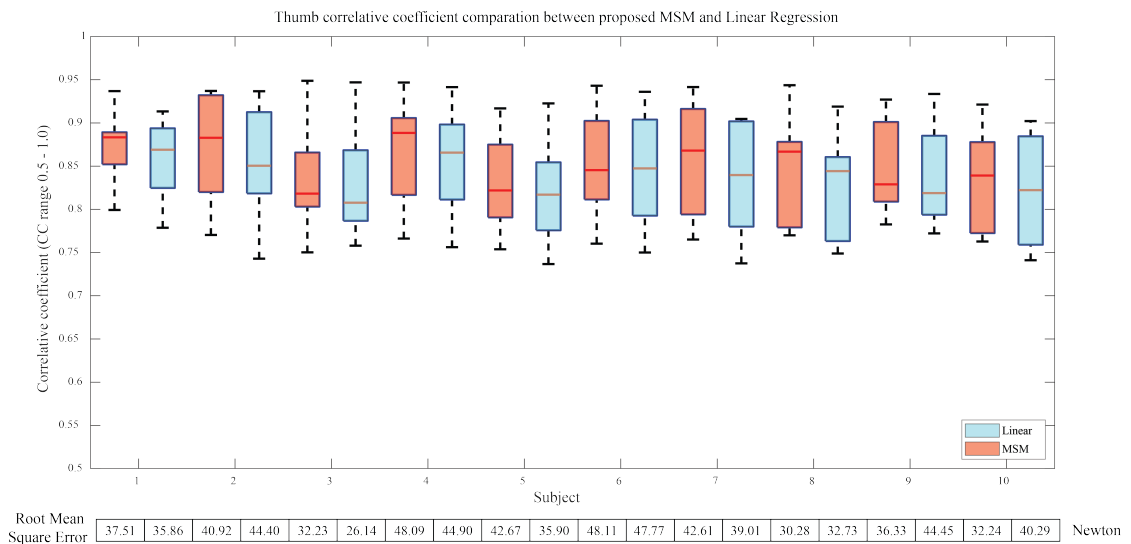


Figure 3.10: Finger force correlation and RMSE between estimated force using musculoskeletal model, linear regression, and measured force using ReachMan Robot.

on one subject. However due to muscles fatigue, we try to limit the number of repeated experiments to as small as possible for each subject.

The results of MSM and LRM in force were not different because the relation between EMG signal and force from finger was linear. Therefore, MSM did not provide any advantage over LRM.

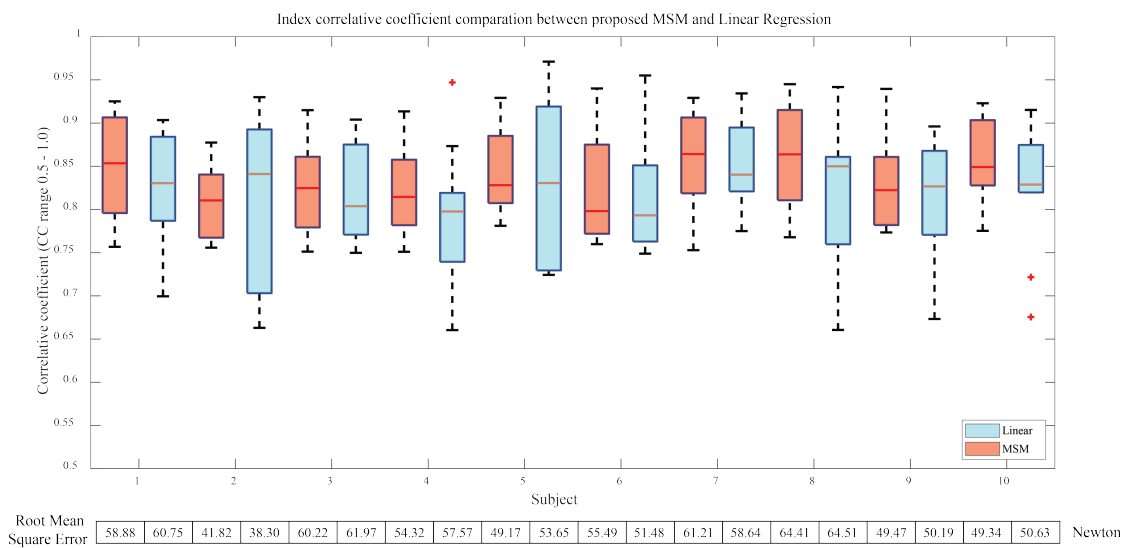


Figure 3.11: Finger force correlation and RMSE between estimated force using musculoskeletal model, linear regression, and measured force using ReachMan Robot.

Chapter 4

Array sEMG system for deep muscles investigation.

After regression method was confirmed using musculoskeleton model and conventional Surface ElectroMyoGraphy (EMG) sensor. Many problem was arise as followed.

- sEMG sensor needs to be directly above the joint control muscles and also align with muscle direction. This leads to rejecting some of the subjects who have too large wrist muscles and we cannot find the location for finger muscles.
- During the experiment, subjects must not changes posture or rotate the wrist. This changes the location of muscles and in some cases, the experiment needs to be redone. The subject was asked to repeat all the processes again if sensors cannot acquire reasonable data.
- Cannot differentiate between wrist and finger muscles due to close proximity. This happened to subject with small arms who have relatively small

finger muscles and cannot find the location in which the EMG sensor can sense those muscles.

- Due to the contamination of the wrist muscle signal, some subjects need to be trained to control the finger without co-contraction of the wrist.

In order to address such issue, the method inspired by EEG system by place electrodes around the forearm and collect data simultaneously. We called this system array EMG sensors and select only signal that have potential to explain motion. The arm sleeve was made by bio-semi device, 96 channel with distance between electrode, in ventral-dorsal direction 20 millimeters, and radial-ulnar direction 16.6 millimeters.

We using this system with independent component analysis (ICA) and find the best independent component (IC) that match the each finger motions while located inside the anatomical location. We extract IC from EMG signal, then finger angles were estimated from linear regression model (LRM) and musculoskeletal model (MSM). The result was analysis using correlation coefficients (CC) and root-mean-square-error (RMSE) for all fingers. The average CC values were higher than 0.7 with RMSE less than 0.1 demonstrating the strength of the linear relationship. The different in performance of LRM and MSM suggests that the IC method can reduce noise while increase the signal to noise ratio. The result show ICA provide higher CC value at around 0.2 ± 0.10 . The result of this study indicate array EMG sensors with ICA can improve the quality of signal while reduce problems of conventional EMG sensors. This result in raise the performance of regression method to imitate natural finger motion.

4.1 Aim of this section

In this thesis, we proposed a method using array EMG system around the forearm. The EMG signal was processed by ICA to find IC and select IC that activate in the same period and also originated from the same area as indicated by anatomy data. Finally, the estimated finger angle and measured finger angle were statistically compared using correlation coefficients (CC) and Root-mean-square-error (RMSE).

4.2 Methodology

The proposed method using array EMG sensors on the forearm. The arm mask was made with each sensor size around 10 millimeter and placed apart with a distance of minimal 15 millimeter. Pattern of placement was 10 columns horizontally and 5 rows vertically on both sides (100 positions) according to Figure 4.1.

Electrode was placed in a zig-zag pattern to minimize distance between each group of electrode. The electrodes were separated into 2 groups of flexor: A1-A32, C1-C16 (48 channels), and extensor: B1-B32, C16-C32 (48 channels) according to Figure 4.2.

4.2.1 Subjects

In this experiment, we have 10 healthy subjects (7 males and 3 females), age between 24 and 28 years old with a mean of 26.2 and SD of 1.8. The study protocol was approved by the ethics committee of the Tokyo Institute of Technology. The experiment was carried out in accordance with the Declaration of Helsinki. Written informed consent was obtained from each participant before the experiment.

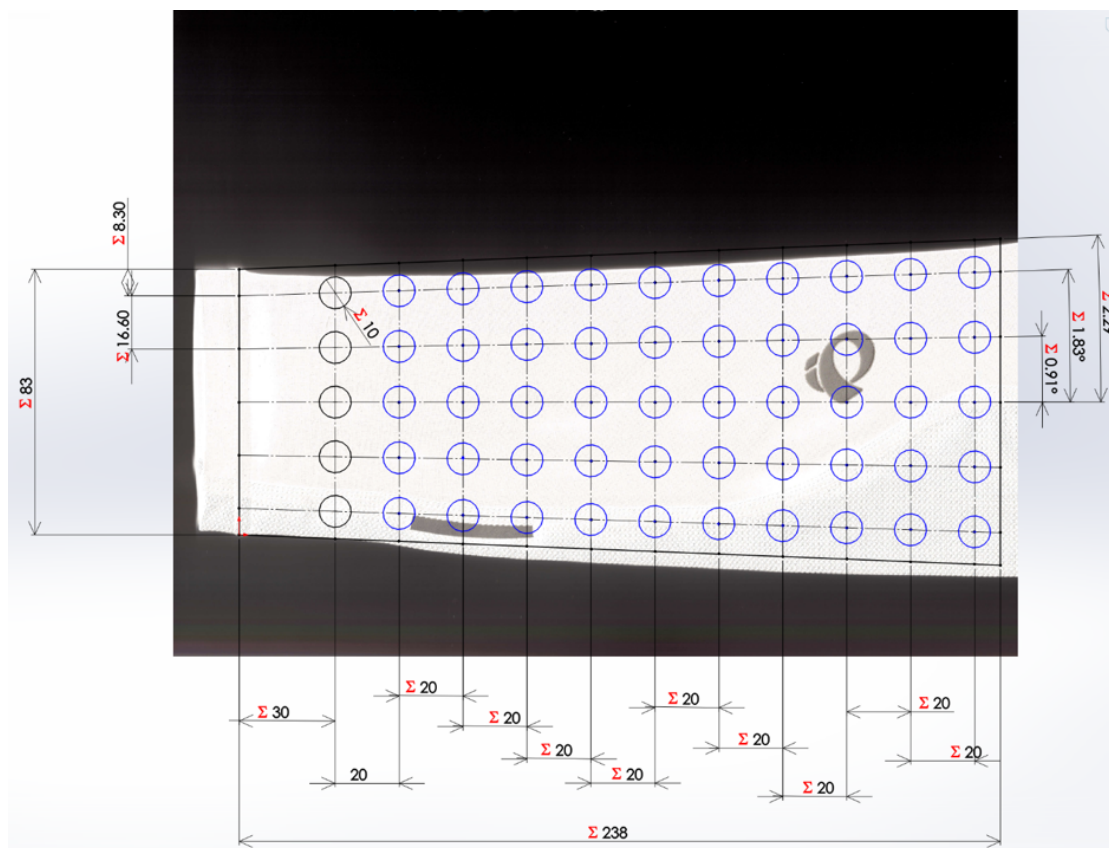


Figure 4.1: The arm mask was made with each sensor size around 10 millimeter and place apart with distant of minimal 15 millimeter. Pattern of placement was 10 column horizontally and 5 row vertically on both side (100 position).

4.2.2 Experiment Protocol

All subject performed 30 experiments of 5 experiments per each finger (Thumb, Index, Middle, Ring, and Pinky) and 5 experiments for test experiments.

We conduct 2 kind of experiment;

- Training experiment to collect data for parameters estimation [16]. The experiment was desired to minimize the cross-talking between different finger muscles to acquire a better EMG signal.
- Testing experiment to collect data for verification of proposed method. The other finger that do not have stimulus was expected to be rest at nat-

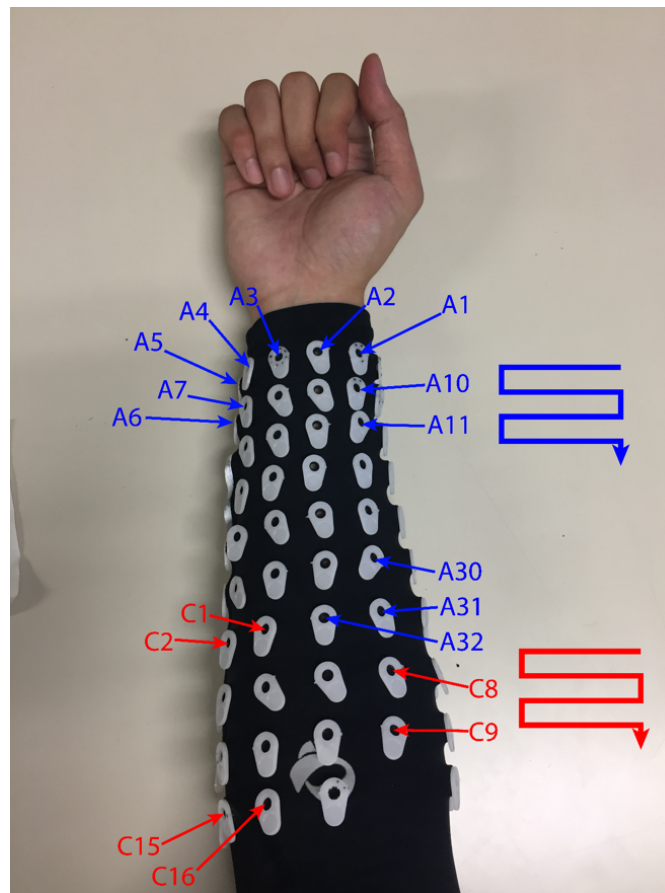


Figure 4.2: The arm mask was made with each sensor size around 10 millimeter and place apart with distant of minimal 15 millimeter. Pattern of placement was 10 column horizontally and 5 row vertically on both side (100 position).

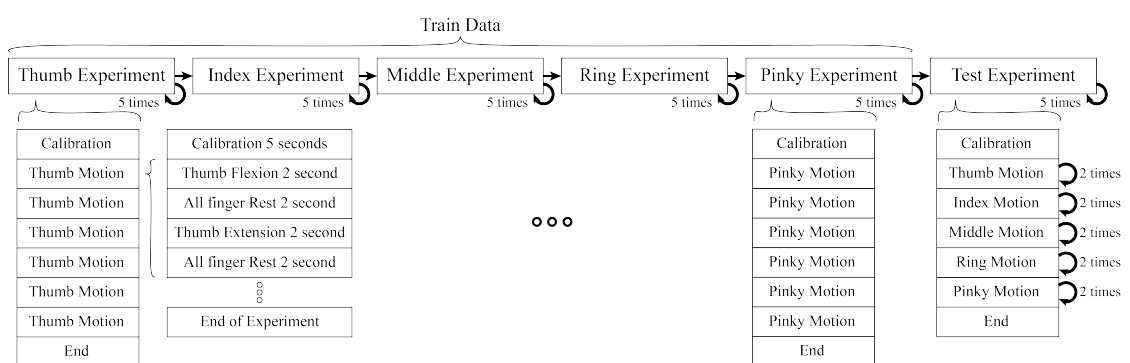


Figure 4.3: Experiment flow for train data and test data, the finger Thumb, Index, Middle, Ring, and Pinky. In flexion, subject flex finger to 0.9 ± 0.175 rad or 162 ± 10 degrees for 2 seconds. rested for 2 seconds, extend finger to -0.20 rad or -36 degree) for 2 seconds, and rested for for 2 seconds.

ural position.

In each train experiments, subject flex finger to 0.9 ± 0.175 rad or 162 ± 10 degrees for 2 seconds. rested for 2 seconds, extend finger to -0.20 ± 0.175 rad or -36 ± 10 degree) for 2 seconds, and rested for for 2 seconds. This cycle was repeated 6 times (see Figure 4.3). In each experiments, there is 5 second calibration period to detect noise and prepare subject for experiment.

In testing experiment, only 1 finger is move to 0.9 ± 0.175 rad or 162 ± 10 degrees for 2 seconds. rested for 2 seconds, extend -0.20 ± 0.175 rad or -36 ± 10 degree for 2 seconds, and rested for another 2 seconds. This cycle was repeated 2 times per experiment.

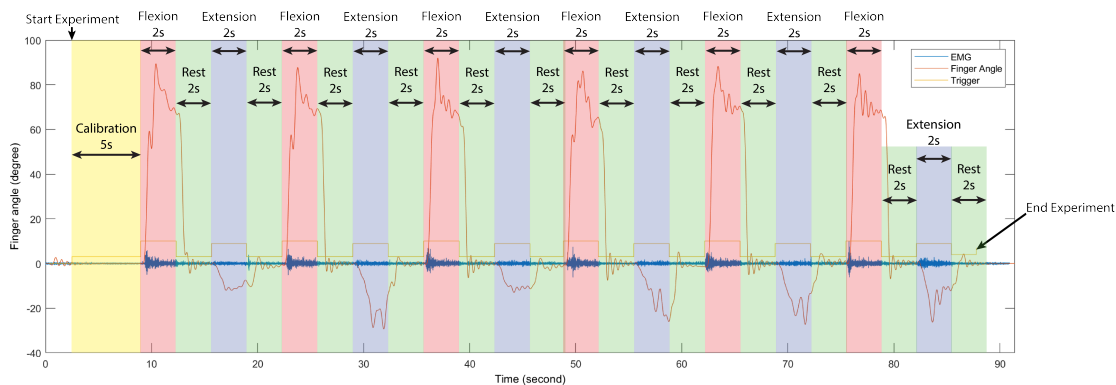


Figure 4.4: Example time serial data. Each section of graph show the separation using stimulus signal (trigger).

In case of interconnection between finger muscles lead to motion of other finger. For example, When attempting to move the ring finger, it is likely to cause movements in the middle and pinky fingers. This following our aim to study the natural motion of human finger. Therefore, the subjects were instructed to not attempting to resist the motion of other fingers.

4.2.3 Independent Component analysis (ICA)

Independent Component Analysis separates independent sources linearly mixed in multiple sensors. We assumed that the signal from the muscles should be

scattered to multiple sensors that located around the forearm, this method was used to extract the EMG signal of muscle groups that corresponded to flexion and extension period of interested fingers.

EMG was sampling with 2000 Hz, band-pass filtering between 5 Hz and 200 was applied. the data were resampled to 500 Hz to reduce computational time. The calculate done in MATLAB with MoBILAB toolbox⁵¹. The EEGLAB version 15 (<https://sccn.ucsd.edu/wiki/EEGLAB>) was used to interact with ICA algorithms and EMG data. From several ICA in EEGLAB, we select adaptive component analysis (AMICA) according to these features [24]:

- Adaptive Source Densities
- Multiple / Mixture Models
- Data Likelihood (Model Probability)
- Parallel Implementation

All calculation was perform with the same machine as previous chapter 4.

With my IC, this cause problem of how to pick a appropriate IC for each muscles.

To understand the source of IC signal, we illustrate the weight of IC in spatial space and compare it with anatomical data.

To determine the source of the IC signal, we compared its location with the anatomical data. The weight was plot on 2D space and changes value into color of blue to red as shown in Figure 4.5. Channel A1-A32 and C1-C16 corresponded to the left side as mostly flexor. Channel B1-B32 and C17-C32 corresponded to the right side as mostly extensor.

Only 16 IC with top score CC value will be displayed with its topology plot to remove noise. The best IC was found from the location that correlate to the general anatomy data (see Figure 4.6).

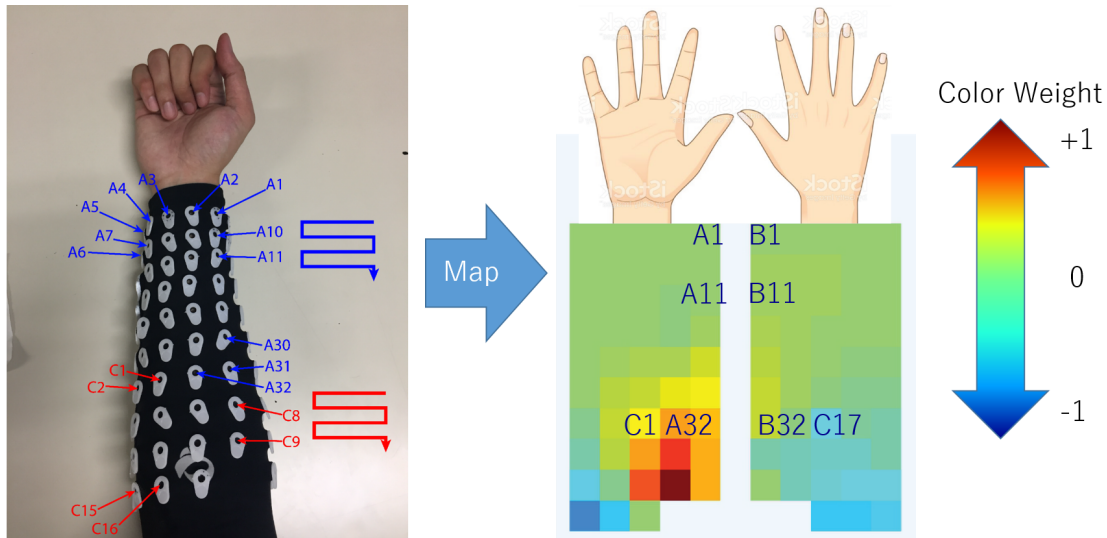


Figure 4.5: Configuration (July 2018) of topology plot for show IC weight as color from -1 (blue) to 0 (green) to 1 (red). Identify the source of IC data on the spatial array EMG system. Topology plot find and match the relation between weight of IC and electrode channel.

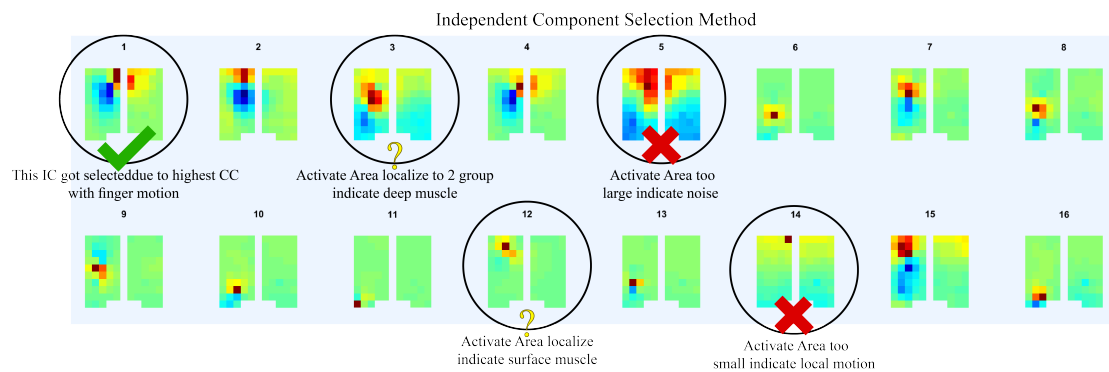


Figure 4.6: 16 IC with top score CC value.

4.2.4 Topology plot to investigate spacial data of independent component (IC)

The topology plot shows spatial data of the weight of the independent component (IC) in sensors. Topology plot consist of 2 part which shown sensor

located in flexion (inner arm) and extension (outer arm) groups. These group was rearrange to left and right side, respectively as shown in Figure 4.5.

The bio-semi electrodes were separated into a group of 4 electrodes with a maximum distance between electrodes of 15 centimeters, therefore, electrodes were arranged in a S pattern to compliant. The image of the topology plot also replace channel labels with the relative geometry location of sensors on the forearm and from here onward, we will describe the topology in term of array EMG area not channel labels.

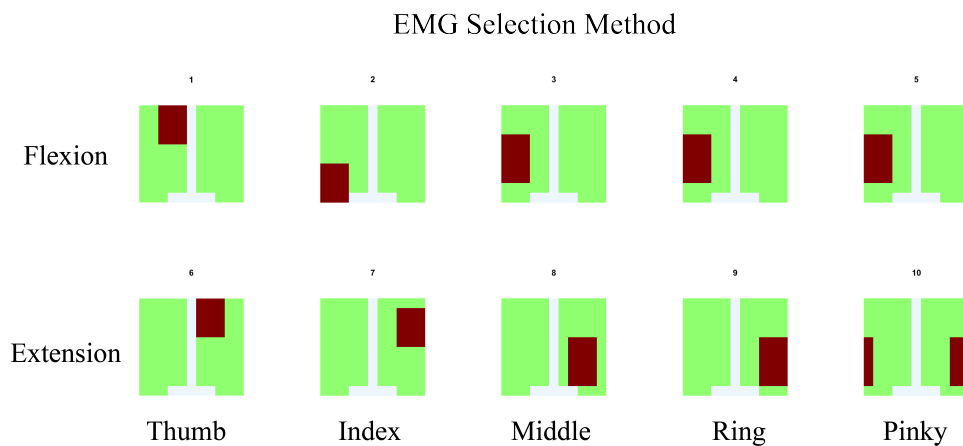


Figure 4.7: The general location of muscles activation according to anatomy data according to finger motion (flexion and extension) and finger.

The EMG signals representative was selected by separate the signal from area according to The general location of muscles activation according to anatomy data according to finger motion (flexion and extension) and finger (see Figure 4.7). Each channel signal was compare with the finger motions for correlation coefficient (CC) to find the electrode that provided the best-fitted pattern between EMG signal and finger motions.

4.2.5 Selection of IC data

This section explained in deed how we select each IC to represent finger flexor and extensor.

intuition

We check time serial data and spacial data of each IC, for example, 32 IC from thumb flexion and extension. Time serial present in Figure 4.8 and spacial data present in Figure 4.9.

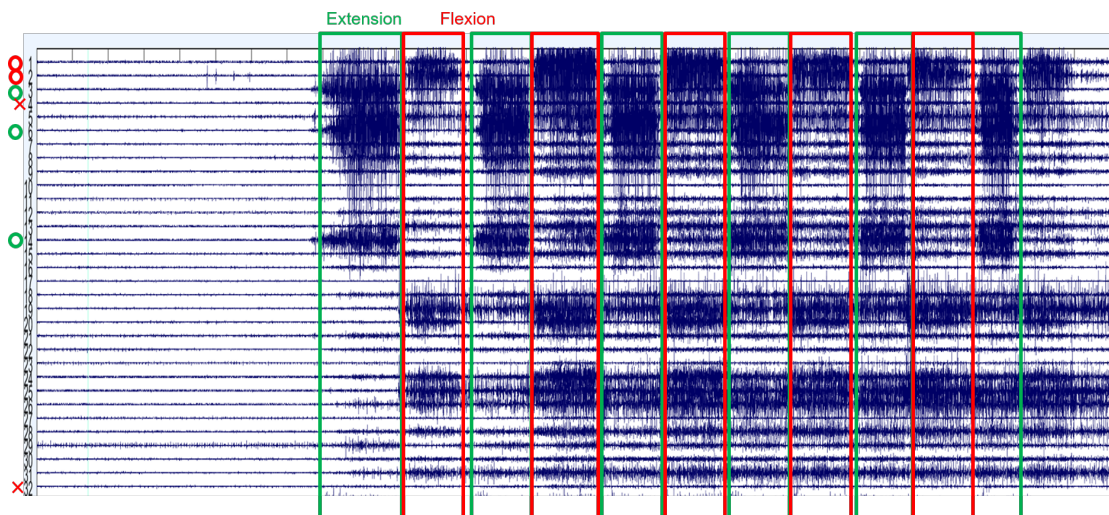


Figure 4.8: Time serial show the period of flexion and exntension of 32 IC from thumb flexion and extension motion

After we plot all of weight of first 32 IC, we can observe the spatial data of each IC and can estimate roughly where the signal came from.

For this dataset of thumb flexion and extension motions. The location of thumb flexor should be around top right of the left panel which related to component 1 and 2, While the location of thumb extension should be around middle right of the right panel which related to component 3, 6 and 14

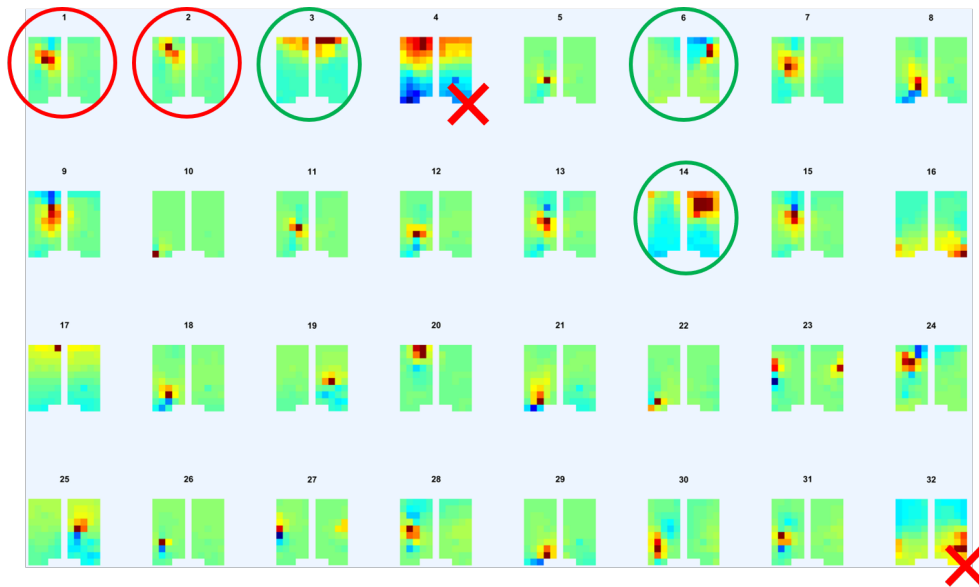


Figure 4.9: Topology plot show the location of 32 IC from thumb flexion and extension motion

If the signal show location in expected area and activation pattern going according to experiment expectation, we considering it potent for represent that muscles. We checked and confirmed that component 1 and 2 were activate in flexion period. Likewise, component 3, 6 and 14 were activate in extension period. Lastly, component 4 and 32 were unable to confirm the activation period which indicate noise signal.

Confirm of muscles location using anatomy data

We investigate the anatomy data to show our result is correct.

The muscles we interest in this section consist of 5 muscles:

- 2. Flexor carpi radialis muscle (Wrist Flexor)
- 6. Flexor digitorum superficialis Muscle (Finger Flexor, intermediate layer muscles)
- 14. Flexor carpi ulnaris muscle (Wrist Flexor)

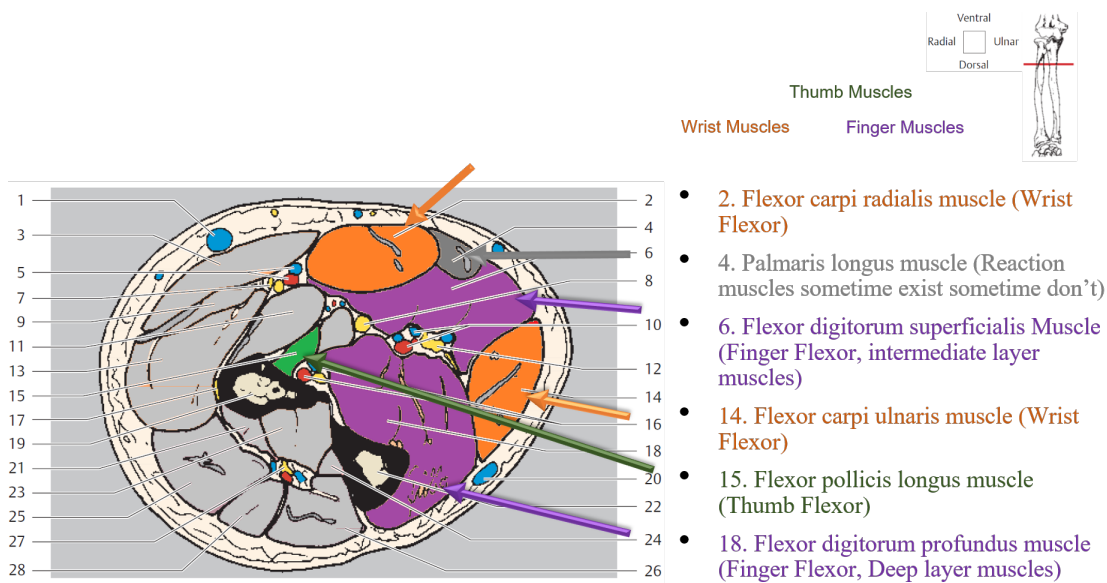


Figure 4.10: Identify the different between wrist and finger muscles signal. We check the location of muscles using anatomy data, we found. 2 wrist muscles, 2 finger muscles, and 1 thumb muscles.

- 15. Flexor pollicis longus muscle (Thumb Flexor)
- 18. Flexor digitorum profundus muscle (Finger Flexor, Deep layer muscles)

as shown in Figure 4.10.

The sensor we expected to receive the signal was, for finger muscles, sensor in row B1, A1, A2 (Flexor digitorum superficialis Muscle, intermediate). Sensor in row A5, and B5 (Flexor digitorum profundus muscle, deep muscles). For wrist muscles, Sensor in row B1, A1, A2 (Flexor carpi radialis muscle). Sensor in row A3, and A4 (Flexor carpi ulnaris muscle) as shown in Figure 4.11.

The time serial data was used to find component which activate in gripping period as shown on Figure 4.12 and 4.13.

Match the component with topology plot as shown on Figure 4.14. We can assume that component 1, 5, and 9 was Flexor digitorum profundus muscle

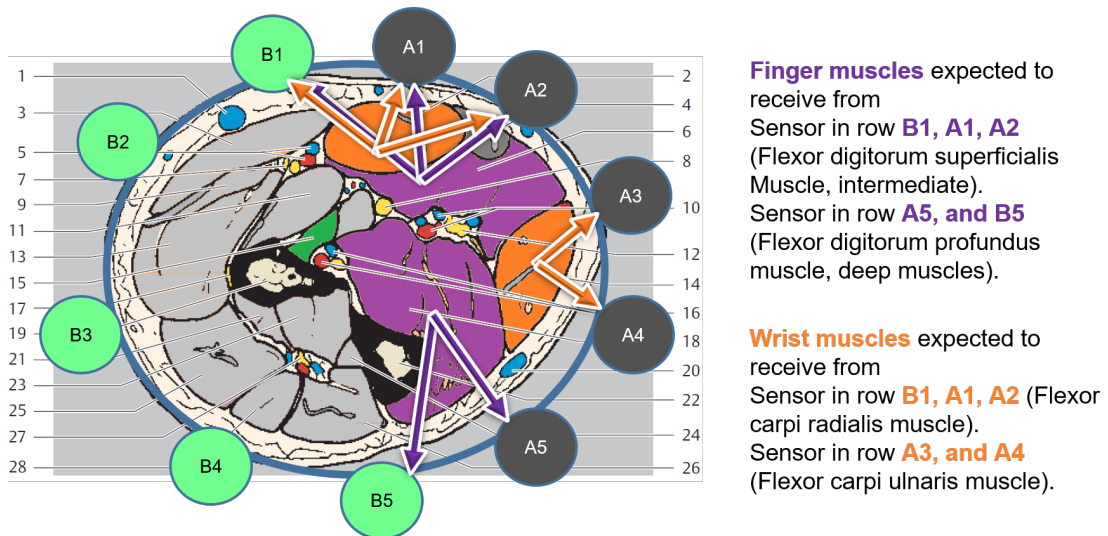


Figure 4.11: We add the sensor number to represent which sensor row should respond to that muscles.

(Finger Flexor, Deep layer muscles) and component 27 was Flexor digitorum superficialis Muscle (Finger Flexor, intermediate layer muscles).

In case of more than IC match the muscles, we select IC with highest signal to noise ratio.

Dipole signature

As we check the topology plot, we can observe most component follow dipole from ICA in EEG analysis as shown in Figure 4.15

We can observe some distant between highest and lowest weigh value, this also indicate di-pole data of component. This might indicate deep muscles.

4.2.6 Finger angle tracking using realsense camera with convolutional-pose-machine

In order to find finger angle, at the time of experiment we do not have method to extract all 5 fingers angle simultaneously. We use convolutional-pose-machine

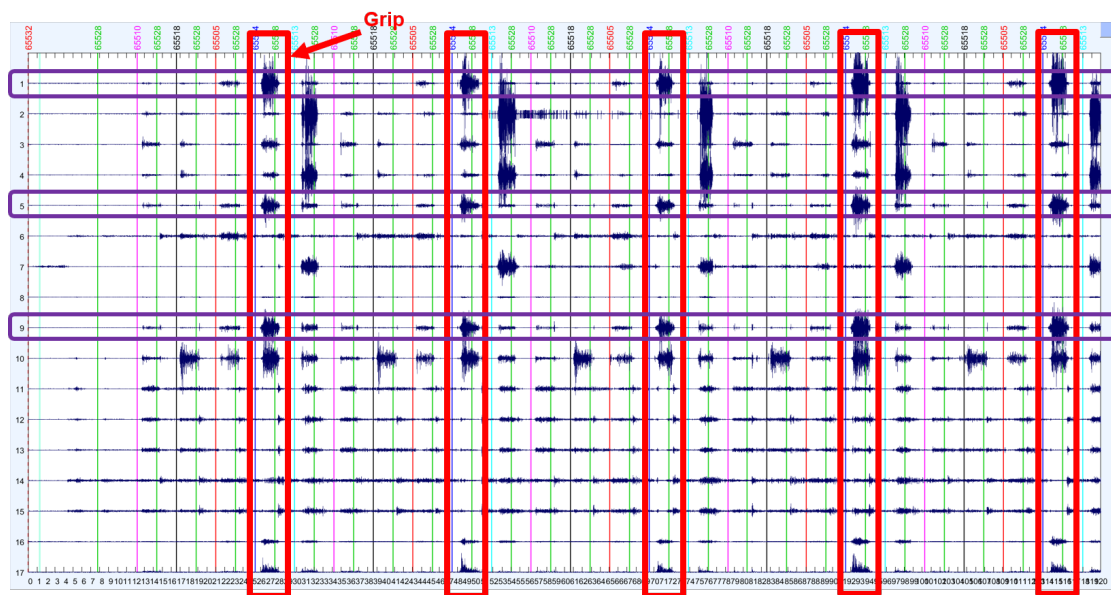


Figure 4.12: IC activation in time serial with indicate griping period and component 1, 5, and 9 which we interested.

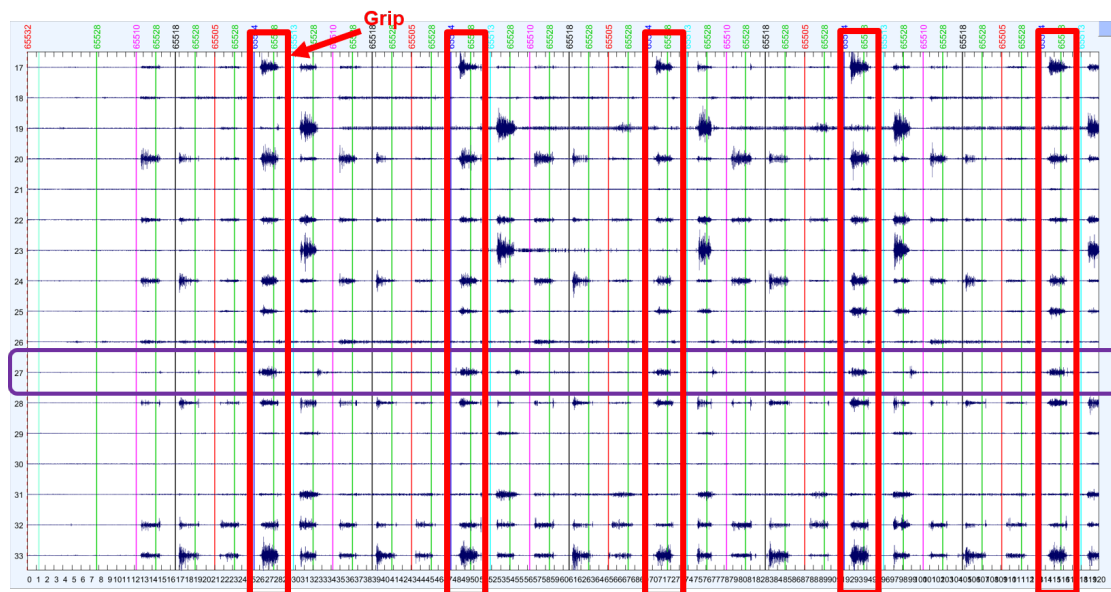


Figure 4.13: IC activation in time serial with indicate griping period and component 27 which we interested.

[37] on realsense camera to extract ground-truth measurement, a state-of-the-art posture estimator. The model was remodel to improve performance by add depth layer with image from Realsense depth camera. The training process using joints' 2D position from the five fingers. In calibration period, all finger was record nominal range of each finger as shown in figure 4.4. Then we applied

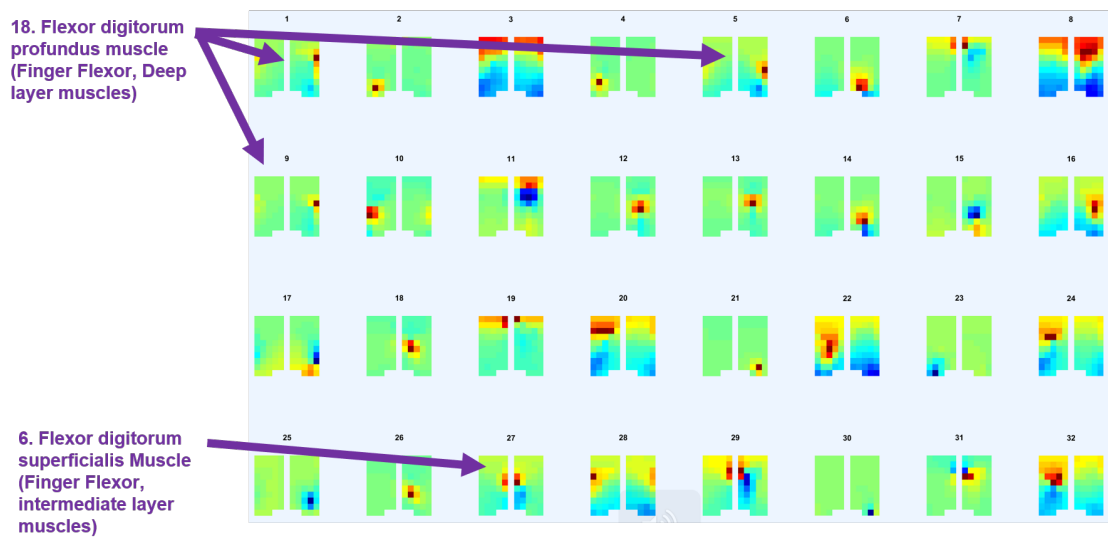


Figure 4.14: The topology plot of component 1, 5, 9, and 27.

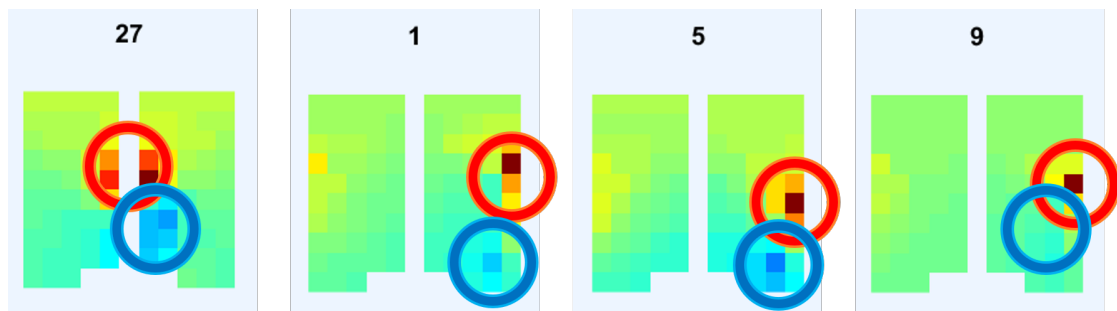


Figure 4.15: Topology plot from IC that might indicate deep muscles.

low-pass filter with cutoff frequency of 1 Hz to reduce noise during posture estimation.

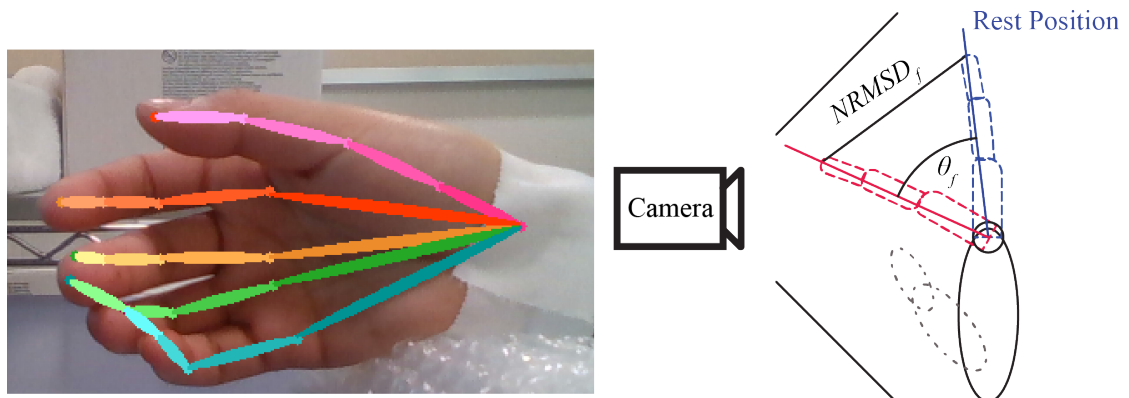


Figure 4.16: Left: example of data from convolutional-pose-machines. Right: the finger angle was defined as normalized root mean square error (NRMSE) in 2D space.

Finger angle (θ_f) was calculated from direction indication of trigger (T_{dir}) which provide the direction of flexion and extension in finger angle and normalized root-mean-square error (NRMSE) as shown in Equation 4.1. The maximum of flexion and extension motion that depend on experiment trigger value was 2.094 radian or 120 degree and -0.523 radian or -30 degree, respectively.

$$\theta_f = T_{dir} \cdot NRMSE_f \quad (4.1)$$

The low-pass filter was applied to reduce noise in estimated finger positions before calculate normalized root-mean-square error (NRMSE). The rest period data also used to adjust the nominal range of each finger to reduce static error due to subjects moved their hand out of detection range. The subject was asked to perform section of experiment again if the convolutional-pose-machines could not track finger or loss track while experiment was conducted.

Optitrack thumb, index, and pinky finger tracking system was used to confirm the performance of the realsense camera with convolutional-pose-machine's finger tracking. The optitrack was setup in Baseline Upper Body + Fingers (33) to extract thumb, index, and pinky finger angle in 3D space while was normalized into 2D space data (axis on the hand direction and palm). Thus, we compare only 3 fingers to evaluate the performance between convolutional-pose-machine and the Optitrack system. The result showed an average R^2 of 0.87 with CC at 0.9040 ± 0.1 , this implied that the convolution-pose-machine provides an accurate ground-truth measurement of the finger angles.

4.2.7 Data acquisition

The subjects were sat in front of screen that given instructions. The screen to subject distant is 50 centimeters with SD of 20 centimeters according to subject arm length. Right hand was place in front of realsense camera to capture finger motions. The array EMG system was attached to subjects' right forearm.

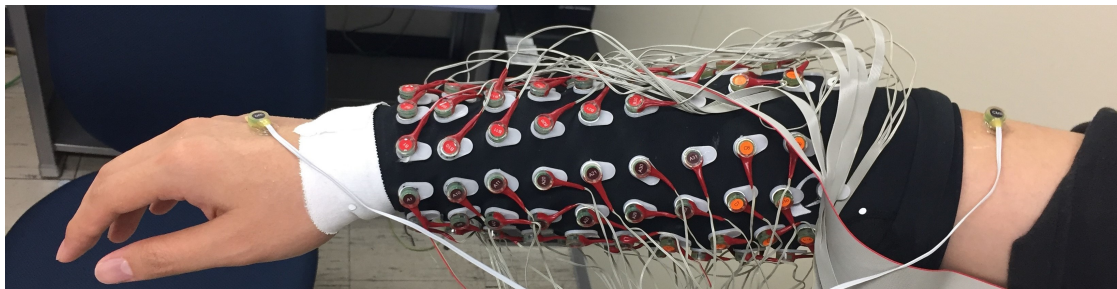


Figure 4.17: Example of bio-semi electrode sensor in first experiment, other experiment also use the same pattern, please notice the CMS and DRL electrodes. The location of this electrodes need to changes according to subject with 1. on the back of hand 4 centimeters apart, 2. between the hand and upper arm, 3. in position A26 and B26.

Data was acquired as follow:

- EMG signal: Biosemi Active Two, 24-bit resolution, sampling rate: 2048 Hz.
- Finger angle was estimated using realsense camera with convolutional-pose-machine with sampling rate of 100 Hz.
- The experiment stimulus work in MATLAB 2015b (The MathWorks, Inc., U.S.A.) program.
- Lab Streaming Layer [20] synchronize the EMG, finger angle, and experimental stimulus.

EMG signals sampling at 2048 Hz, The electrodes were separated into three groups: Group A represented mainly flexion muscles located in the inner forearm; Group B represented mainly extensor muscles, which are located in the

outer forearm; Group C was optional for the subject who has long arm and were separated into two groups of 16-flexion and 16-extension electrodes. In case of CMS and DRL electrodes, the location of this electrodes need to changes according to subject with 1. on the back of hand 4 centimeters apart, 2. between the hand and upper arm, 3. in position A26 and B26 as shown in Figure 4.17.

4.2.8 Finger angle regression model

Musculoskeletal Model (MSM)

Musculoskeletal model (MSM) was a second order regression with constrain to control the variable according to Mykin model [30].

Linear Regression Model (LRM)

Linear Regression Model (LRM) was a first order regression without constrain.

4.2.9 Performance Indicators

In this study, we used representatives of performance for our proposed system using performance indicators. The representatives are correlation coefficient (CC) and Root-mean-square-error (RMSE) with mean and standard deviation according to section 3.3.2.

4.3 Results

The monopole EMG signal was collect from 96 channel Bio-semi sensor. Raw signals was re-reference (using average reference) and band-pass filtering between 5 Hz and 200 Hz to reduce noise [29]. The EMG channels was select for each finger muscles with 2 criteria:

- EMG channels has to be within the area where we expect the muscle to be located as shown in Figure 4.7;
- That channel has the highest correlation between EMG signal and ground-truth finger motion.

Next ICs was calculated from all EMG channels using AMICA. After AMICA, the EMG and IC signals were rectified and low-pass with cut-off frequency of 3 Hz according to [19]. The IC was select for each finger muscles with multiple criteria according to Figure 4.6.

The train data of EMG, IC, and finger angle was used to find muscles parameters for MSM and beta variables for LRM. Then, we used those parameters and variables to estimate finger angle from each method (see Figure 4.18). These estimation were compared with the ground-truth finger angles from the convolution-pose-machine to calculate the CC and RMSE (see Figure 4.19). The result from MSM and LRM was used to test the hypothesis that CC and RMSE of IC and EMG method were statistical significantly different, a paired t-test was used. The p-values of CC and RMSE between IC and EMG were below 0.05 which considered statistically significant.

To reduce complexity, the analysis result of MSM using EMG and IC will be called MSM-EMG and MSM-ICA, respectively. Likewise, the analysis result of LRM using EMG and IC will be called LRM-EMG and LRM-ICA, respectively.

Figure 4.20 and Figure 4.21 shown CC in boxplot and RMSE in barplot average and SD from all subject for each finger. MSM-ICA was represented with red area, MSM-EMG was represented with green area, LRM-ICA was represented with yellow area, LRM-EMG was represented with blue area.

The first analysis used 5 train data experiments to find finger muscle param-

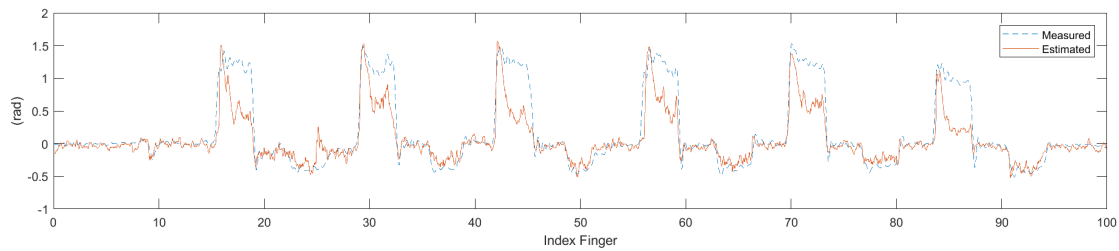


Figure 4.18: Example of time serial data of index finger between estimated using MSM and measurement from realsense camera with convolutional-pose-machine.

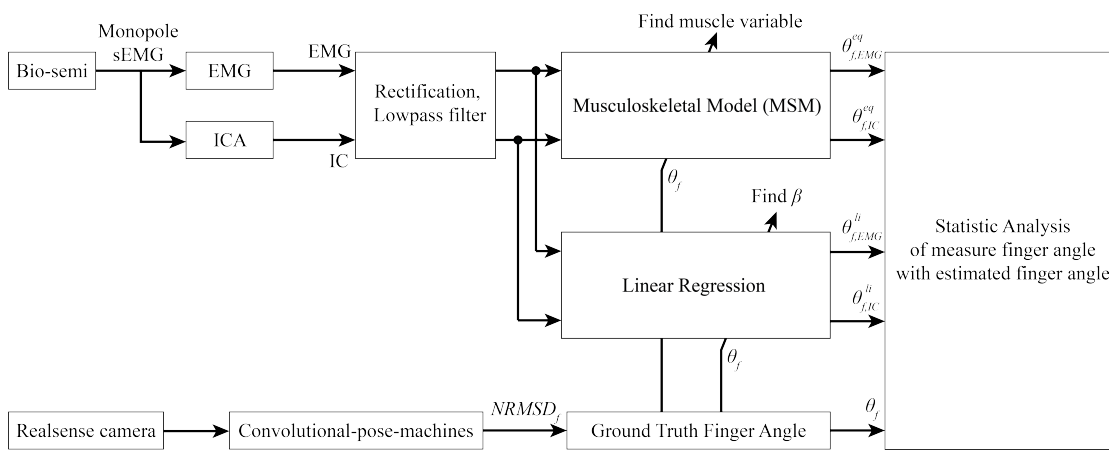


Figure 4.19: Research analysis flow.

eters for MSM and variables for LRM. The model was validated using 5 test data experiments (see figure 4.20) and statistical analysis. This analysis show the performance of proposed method in case of abundance dataset can be acquired. Therefore, the performance was expected to be high.

The second analysis used 1 test data experiments to find finger muscle parameters for MSM and variables for LRM. The model was validated using 4 test data experiments (see figure 4.21) and statistical analysis. This analysis show the performance of proposed method in case of small number of dataset was acquired. Therefore, the performance was expected to be lower than first analysis. 5-fold validation was adapted to ensure non-bias result.

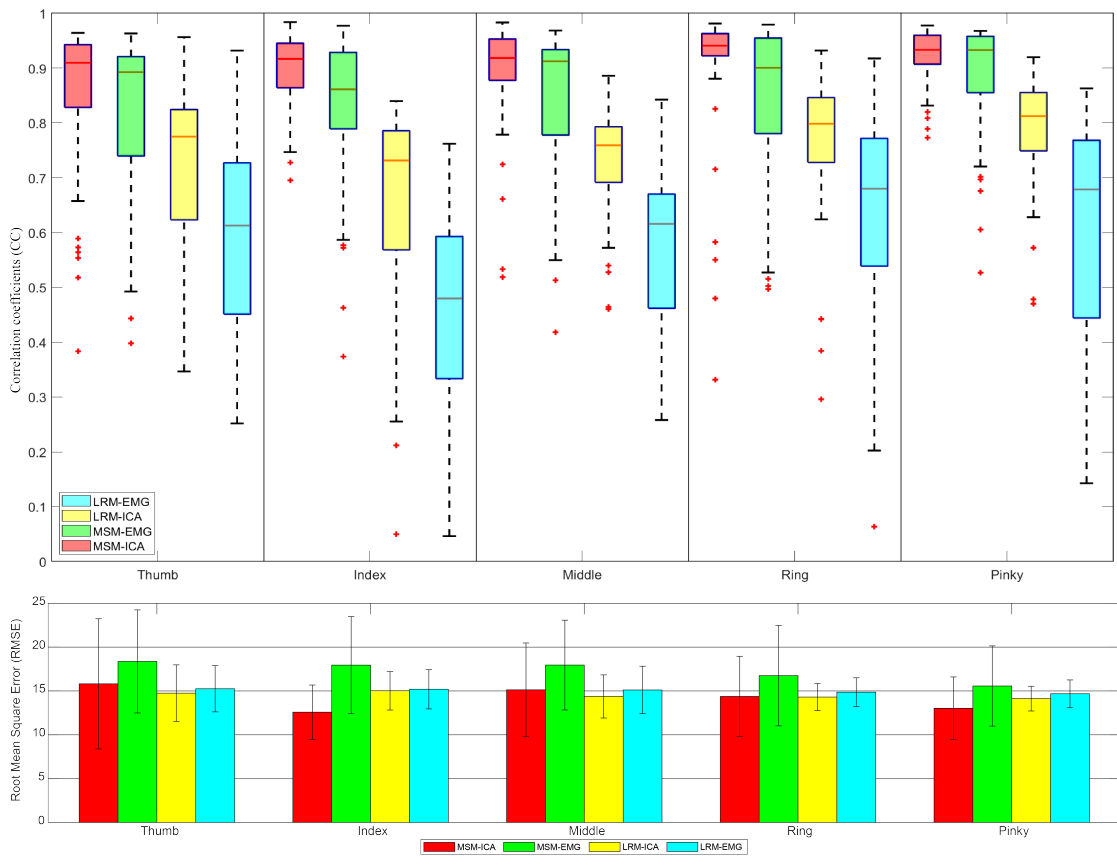


Figure 4.20: Performance of proposed method in first analysis: 5 train data for training and 5 test data for testing. The correlative coefficient was in boxplot and root-mean-square-error in barplot. number of data = 50 (10 subjects * 5 tests).

4.4 Discussion

The performance of ICA and EMG show almost 0.1 better in ICA. Meanwhile MSM and LRM show better performance in both CC and RMSE for MSM. The different between MSM and LRM were explained by the second order of MSM help in regression for finger angle. The different between ICA and EMG were explained by the robustness of the ICA approach to reject noise and motion artifacts compare to EMG signal. Table 4.1 provide summary each finger CC and RMSE for each method on 2 analysis.

The first analysis (Figure 4.20) confirm the result in optimal situation, MSM-EMG with average CC value at 0.90 ± 0.30 with high signal to noise ratio EMG

Table 4.1: Summary of average statistic value from 10 subjects of Figure 4.20 and Figure 4.21, foe reference.

Exp	Value	Thumb		Index		Middle		Ring		Pinky	
		IC	EMG	IC	EMG	IC	EMG	IC	EMG	IC	EMG
MSM train	CC mean	0.86	0.80	0.94	0.80	0.91	0.85	0.91	0.86	0.94	0.89
	CC std	0.18	0.17	0.04	0.19	0.09	0.13	0.11	0.15	0.04	0.11
V test	RMSE mean	15.81	18.36	12.58	17.95	15.13	17.95	14.38	16.75	13.02	15.56
	RMSE std	7.43	5.88	3.10	5.54	5.35	5.12	4.57	5.73	3.58	4.57
LRM train	CC mean	0.73	0.60	0.66	0.46	0.73	0.57	0.77	0.64	0.79	0.60
	CC std	0.13	0.18	0.18	0.17	0.11	0.16	0.13	0.19	0.10	0.20
V test	RMSE mean	14.8	15.3	15.0	15.2	14.4	15.1	14.3	14.9	14.1	14.7
	RMSE std	3.22	2.64	2.19	2.24	2.46	2.71	1.55	1.64	1.41	1.58
MSM test	CC mean	0.84	0.67	0.80	0.65	0.86	0.68	0.86	0.77	0.91	0.73
	CC std	0.14	0.23	0.19	0.21	0.10	0.19	0.17	0.19	0.06	0.26
V test	RMSE mean	10.0	13.7	10.4	13.1	9.7	13.9	8.9	10.5	7.3	12.8
	RMSE std	6.04	6.16	7.10	5.43	6.23	6.19	5.64	4.94	1.80	7.30
LRM test	CC mean	0.73	0.61	0.71	0.48	0.73	0.55	0.78	0.68	0.82	0.62
	CC std	0.18	0.17	0.17	0.20	0.11	0.15	0.13	0.18	0.08	0.12
V test	RMSE mean	12.2	14.8	11.7	15.4	14.1	15.1	10.3	12.1	9.8	14.4
	RMSE std	5.47	6.55	4.12	6.78	9.21	6.04	2.88	3.50	2.75	7.85

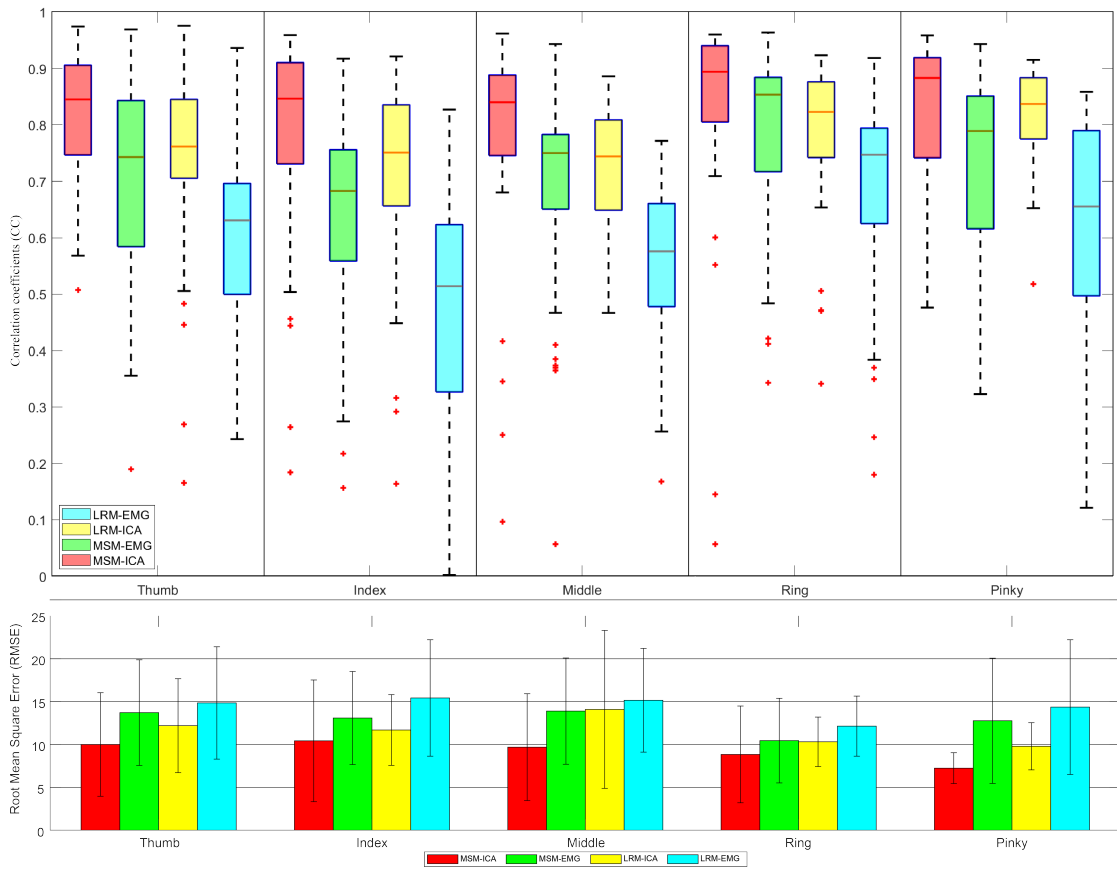


Figure 4.21: Performance of proposed method in second analysis: 1 test data for training and 4 test data for testing. 5-fold validation was adapted to ensure non-bias result. The correlative coefficient was in boxplot and root-mean-square-error in barplot. number of data = 50 (10 subjects * 5 tests).

signal. This clearly show distinguishable activation pattern. While LRM-EMG performed worst with average CC value at 0.55 ± 0.05 because of the relation between EMG signal and finger angle was not single order linear. RMSE also showed higher value in MSM method average 2.0 degree. However, the impact of ICA method still visible in comparison and as a result. MSM-ICA showed the best performance from all proposed method.

The second analysis (Figure 4.21) confirm the result in real situation where er have limited data. The performance of MSM showed lower CC at 0.70 ± 0.10 and LRM at 0.55 ± 0.10 using EMG signal. While ICA showed significant higher performance and better robustness for MSM and LRM with CC value at 0.84 ± 0.10

and 0.76 ± 0.06 . MSM show best result with lower RMSE of 3.0 ± 1.0 , 2 ± 1.0 , and 4.0 ± 1.0 degree compare to MSM-EMG, LRM-ICA, and LRM-EMG, respectively.

We narrow the interest into ICA and EMG signal by compare only MSM-ICA, MSM-EMG and LRM-ICA, LRM-EMG. The MSM-ICA and MSM-EMG method showed 10% (CC 0.10) increased in CC values and 3.0-5.0 degree lower average RMSE. Every finger have CC more than 0.7 that indicated a strong uphill linear relationship. The LRM-ICA and LRM-EMG method showed 20% (CC 0.20) improved performance with 1.0-3.0 degree lower average RMSE.

These result indicated that ICA method reduce noise and increase signal to noise ratio for MSM model. However ICA method still need human supervision on IC selection process. If the process can be automate, ICA should able to consistently provide better performance.

4.5 Conclusions

In this study, we proposed new method called array EMG system to replace conventional surface EMG sensor. The array EMG system place over forearm by integral Bio-semi and arm mask to detect mono-pole surface EMG signal simultaneously. Muscles EMG signal source can be determined in post analysis. Moreover, the ICA method can be used to find higher quality signal source. The setup time of this system is about 30 minutes with two operators. The proposed method also provided overall better signal quality and other advantage as shown in Table 4.2.

The finger angle was calculated from the NRMSE of convolutional-pose-machines-tensorflow according to the trigger to determine the direction of finger angle (flexion or extension). The EMG signal from flexor and extensor muscles were

Table 4.2: Array EMG system advantage to conventional EMG sensor

	Array EMG system	EMG sensor
Do not need information of muscles location	✓	✗
Do not need predefined number of muscles	✓	✗
Can handle muscles location changes during experiment	Post analysis adjustment	✗
Use ICA to reduce noise	✓	✗
Signal to noise ratio	3.0-100.0	1.2-4.5

selected by highest CC between measured finger angle EMG activation pattern. IC was extracted from all surface EMG signals using AMICA [24]. The EMG and IC was considered as representative of flexor and extensor muscles for each finger. The result of estimated finger angle show relatively higher CC using MSM-ICA and LRM-ICA. Considering the practical application in robotic hand, we designed the experiment so that all fingers move continuously without interruption. The experiment showed lowest CC at 0.7 ± 0.2 using LRM-EMG method. However for amputee subject, the muscle locations can be differ from general anatomy data and might unable to find the best location for finger muscles. The proposed method provided a bypass to collect data from entire area and and estimated the location of muscles post analysis.

Chapter 5

Topology plot of multiple subject.

As we plot the topology plot of each subject, we found some similarities that should provide insight to estimate deep muscles EMG signal. However, large scale studies of these are still lagging and some researchers also said that it should be impossible to estimate deep muscles signal due to high crosstalk of wrist muscles.

5.1 Aim of this section

In this study, we found some interesting results from the previous study that deem should be expressed.

The location of each plot will be reference according to figure 5.1

5.2 Topology plot of each subject

This section will show the topology plot of each subject separated between finger muscles, flexor and extensor.

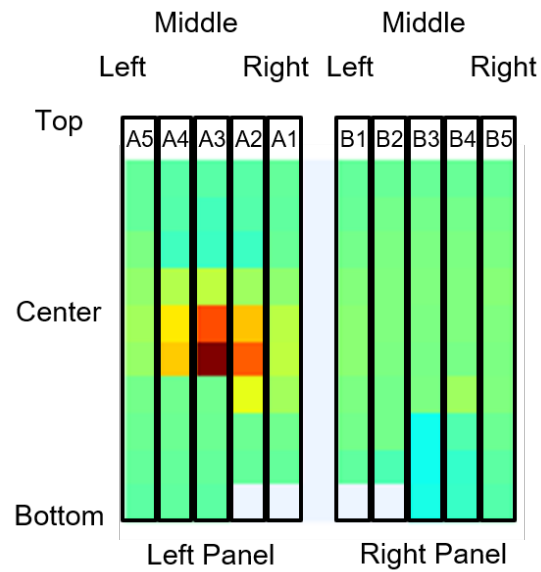


Figure 5.1: Reference to the name of each location in topology plot.

5.2.1 Thumb finger

For the thumb finger, we interested in:

- Flexor pollicis longus muscle (FPL) Figure 2.1.
- Extensor pollicis longus muscle (EPL) Figure 2.3.
- Extensor pollicis brevis muscle (EPB) Figure 2.4.

Compare to our topology plot the flexor should originate from Top-right of the left panel as shown in Figure 5.2.

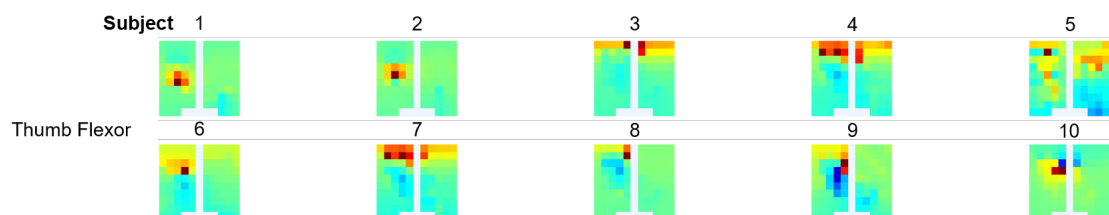


Figure 5.2: Topology plot of thumb flexor from 10 subjects participate in previous study.

Likewise, Extensor should originate from Top-middle of the right panel as shown in all subject of as shown in Figure 5.3.

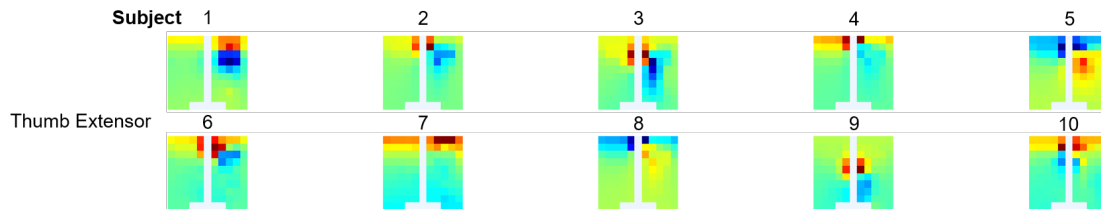


Figure 5.3: Topology plot of thumb extensor from 10 subjects participate in previous study.

Some cross-location also detected, however, that can be explained by the proximity between those muscles.

5.2.2 Index finger

For the index finger, we interested in:

- Flexor digitorum superficialis muscle (FDS) Figure 2.8.
- Extensor digitorum (ED) Figure 2.10.
- Extensor indicis (EI) Figure 2.11.

Compare to our topology plot the flexor should originate from center-right of the left panel as shown in Figure 5.4.

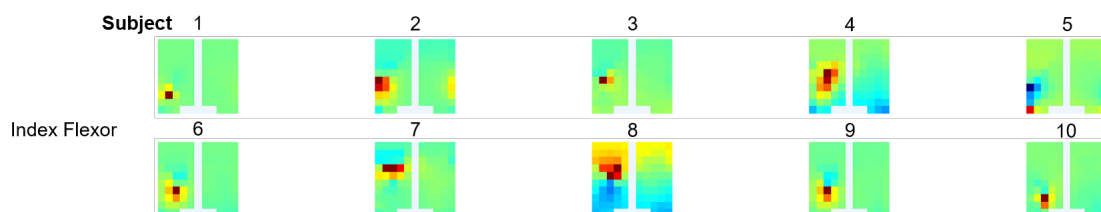


Figure 5.4: Topology plot of index flexor from 10 subjects participate in previous study.

Likewise, Extensor should originate from center-middle of the right panel as shown in all subject of Figure 5.5.

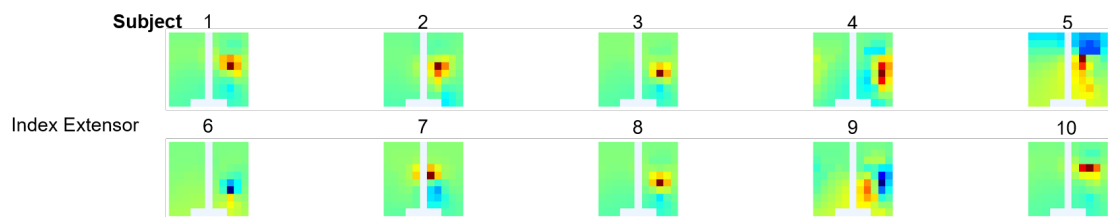


Figure 5.5: Topology plot of index extensor from 10 subjects participate in previous study.

5.2.3 Middle finger

For the middle finger, we interested in:

- Flexor digitorum superficialis muscle (FDS) Figure 2.8.
- Flexor digitorum profundus muscles (FDP) Figure 2.9.
- Extensor digitorum (ED) Figure 2.10.

Compare to our topology plot the flexor should originate from center-middle of the left panel as shown in Figure 5.6.

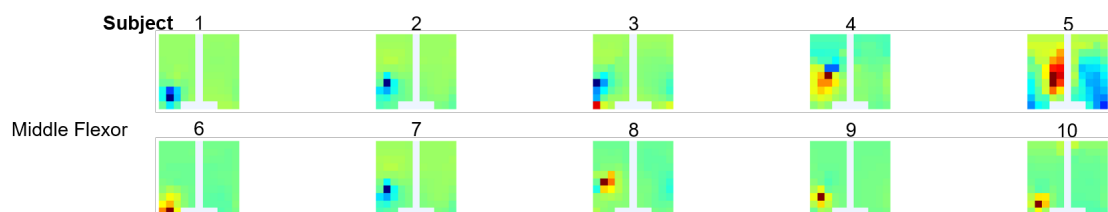


Figure 5.6: Topology plot of middle flexor from 10 subjects participate in previous study.

Likewise, Extensor should originate from center-right of the right panel as shown in all subject of Figure 5.7.

5.2.4 Ring finger

For the ring finger, we interested in:

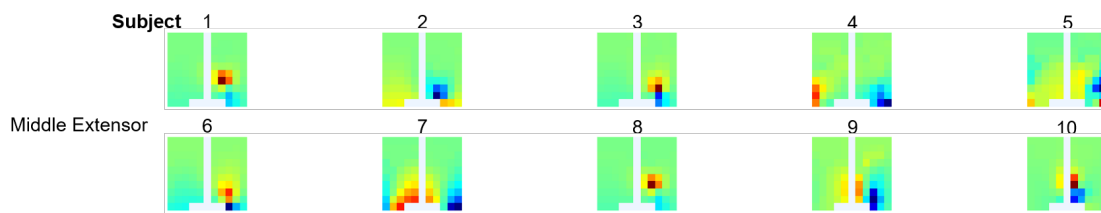


Figure 5.7: Topology plot of middle extensor from 10 subjects participate in previous study.

- Flexor digitorum profundus muscles (FDP) Figure 2.9.
- Extensor digitorum (ED) Figure 2.10.

Compare to our topology plot the flexor should originate from center-left to bottom-left of the left panel as shown in Figure 5.8.

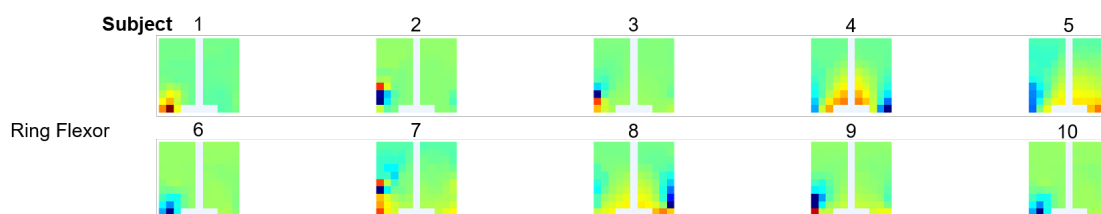


Figure 5.8: Topology plot of ring flexor from 10 subjects participate in previous study.

Likewise, Extensor should originate from center-right to bottom of the right panel as shown in all subject of Figure 5.9.

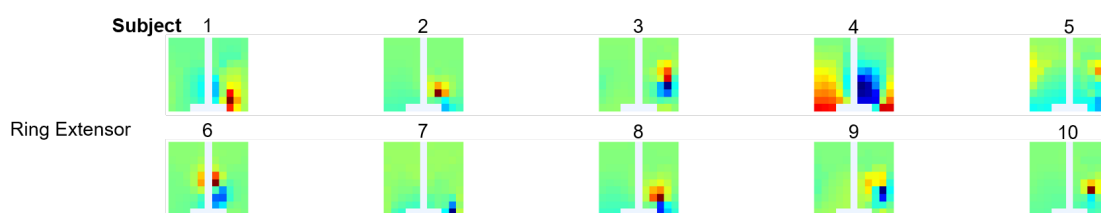


Figure 5.9: Topology plot of ring extensor from 10 subjects participate in previous study.

5.2.5 Pinky finger

For the pinky finger, we interested in:

- Flexor digitorum profundus muscles (FDP) Figure 2.9.
- Extensor digitorum (ED) Figure 2.10.

Compare to our topology plot the flexor should originate from center-left to bottom-left of the left panel as shown in Figure 5.10. Likewise, Extensor should originate from center-right to bottom of the right panel as shown in all subject of Figure 5.11.

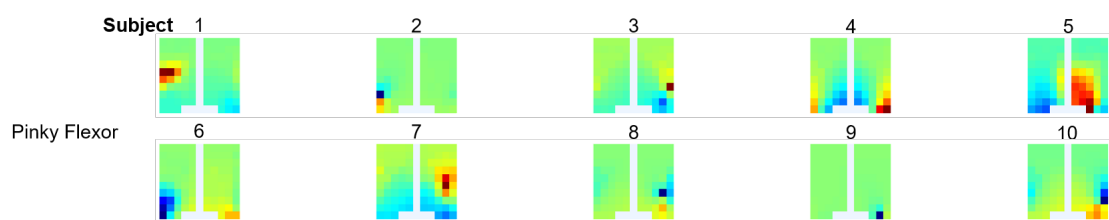


Figure 5.10: Topology plot of pinky flexor from 10 subjects participate in previous study.

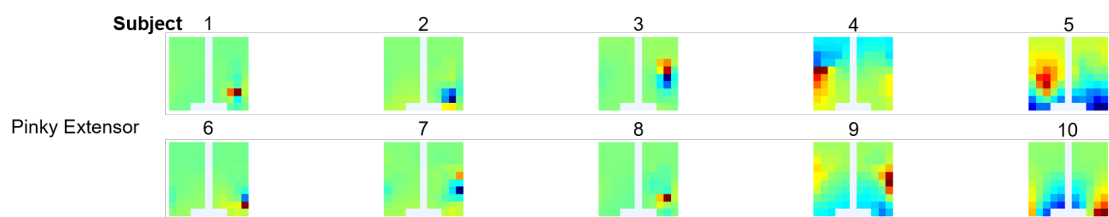


Figure 5.11: Topology plot of pinky extensor from 10 subjects participate in previous study.

The problem was ring and pinky finger have very close result and really hard to separate them. This also reflex in the fact that few people can separately control ring and pinky finger.

5.2.6 Average Result

The average weight of all subject after normalization was shown in Figure 5.12.

The average activation pattern show that, although there is variety of anatomy of each subject but the pattern of signal location still clustered together.

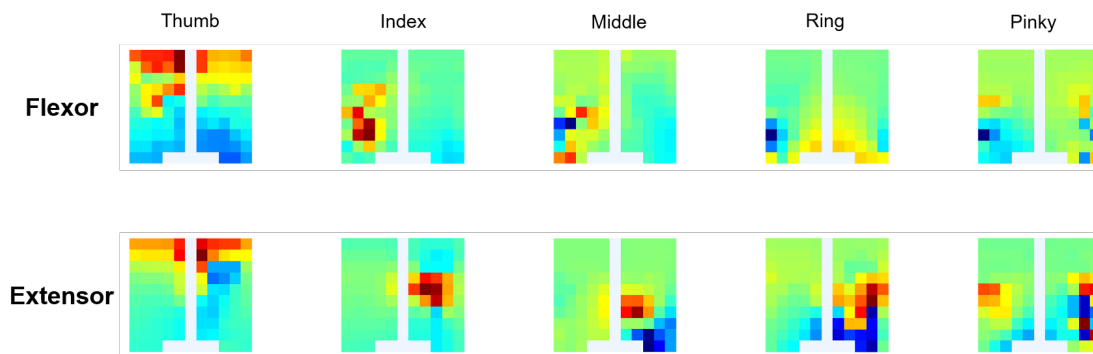


Figure 5.12: Topology plot of average of all subject separate in each finger.

5.3 Dipole of deep muscles signal

We also observe some pattern of dipole from our data. Compare between finger muscles topology plot as shown Figure 5.13 and wrist muscles topology plot as shown in Figure 5.14.

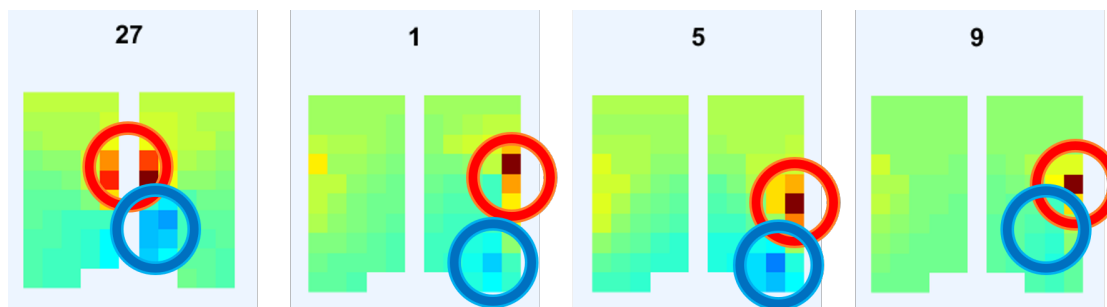


Figure 5.13: Topology plot of component that represent grip and open motion.

The first plot was collect from component that activate during grip motion and small activate in open motion. The distance between highest and lowest weight was calculate by Manhattan distant ($h()$) of vertical was 20 millimeters, and horizontal was 16.666 millimeters.

Averagely, $h()$ of component from first Figure 5.13 (index finger component) was 3.42 times higher than $h()$ of component from second Figure 5.14. This might indicate deep muscles.

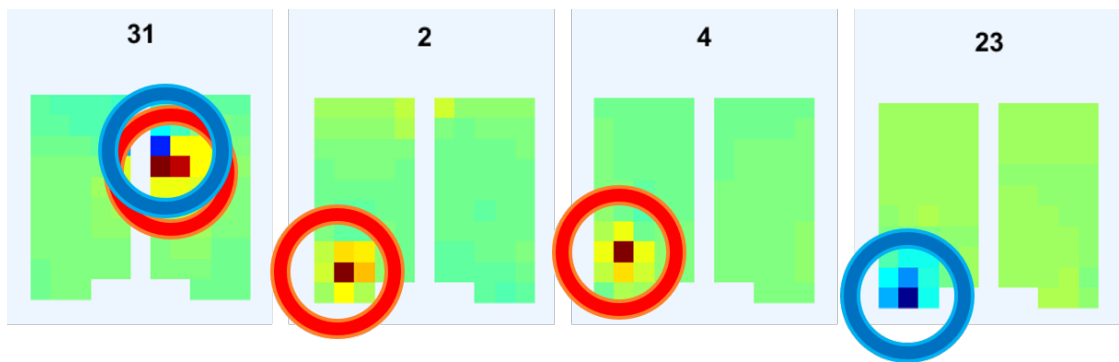


Figure 5.14: Topology plot of component that represent wrist flexion and extension motion.

Chapter 6

Conclusion

6.1 Summary

This dissertation study the possibility to use regression method instead of pattern recognition to estimate finger angle. The start point was musculoskeleton model (MSM) 3.2.1. MSM was a model that able to estimate both joint angle and torque simultaneously. Therefore, the experiment was designed to ensure MSM performance with finger joint.

The result shown that MSM perform better due to 2-order regression but unable to maintain finger angle during smaller activation after motion due to its lack of damper element. The results of MSM and LRM in force were not different because the relation between EMG signal and force from finger was linear. Therefore, MSM did not provide any advantage over LRM.

All of those result have the following problem; according to chapter 3.

1. in order to acquired high quality sEMG signal, sEMG sensor need to be directly above the joint control muscles and also align with muscles direc-

tion. This lead to reject some of subject who have too large wrist muscles and we cannot find location for finger muscles.

2. During experiment, subject must not changes postal or rotate wrist. This changes location of muscles and experiment need to be terminated. The subject was ask to repeat all the process again if sensor cannot acquired reasonable data.
3. Cannot differentiate between wrist and finger muscles due to close proximity. This happened to subject with small arm who have relatively small finger muscles and cannot find the location which EMG sensor can sense those muscles.
4. Due to contamination of wrist muscles signal, subject need to be trained to control finger without co-contraction of wrist. Any dataset which show sign of contamination was rejected and redo the experiment.

We used method inspired by EEG system to measure EMG signal from many position around forearm. We use MSM and LRM to produce naturals finger motion. IC was extract from EMG signal using ICA. Operator pick the best IC that matches general anatomical data. The finger was EMG and IC component for flexion and extension muscles. Each finger angle was estimated and statistically analysis to prove the possibility to produce finger angle separately according to chapter 4.

Our new array EMG sensor provide multiple advantage over conventional devices according to chapter 4.

1. Operator do not need knowledge of muscles location and spend time to find space directly above the joint control muscles and also align with

muscles direction. Post-analysis result shown the signal source generated from approximately correct location of muscles according to anatomical knowledge.

2. We are able to guarantee signal quality during experiment regardless of changing postal or rotate wrist by distribute signal source to area around the target channel. All subjects was able to get high correlation and smaller RMSE without repeat experiment and confirm signal quality after experiment.
3. Using ICA, we are able to achieve better finger muscles signal. However, there are still different between subjects correlate with arm size which smaller show lower signal to noise ratio.
4. Because ICA and PCA are able to separate multiple co-contraction of muscles. All of subject do not need pre-train before the experiment. Decontamination was done in analysis period.

6.2 Aim result

1. **The possibility to changes from conventional pattern recognition system to regression which is the same as musculoskeletal model:** We conduct 2 experiments to estimate finger angle and force from EMG signal. we conclude that it is possible to regress finger angle and force from sEMG signal as long as EMG was high quality.
2. **The method to provide better deep muscles EMG signal by signal processing many sensor around forearm:** In order to achieve better quality EMG signal, we use EMG array system to acquired multiple EMG source at the same time and use post analysis to extract finger EMG signal using

ICA. EMG signal from ICA show much higher quality compare to conventional EMG sensor and also show better performance using the same regression method.

3. **The performance of such method compare with conventional one:** We compare our array EMG system with conventional sEMG method and they show 10% higher CC value and 10% lower RMSE. Therefore, we conclude that array EMG system + MSM provide better performance in finger angle estimation but no different in finger force estimation.

6.3 Future work

1. We would like to develop this system to be automate without operator interaction and ensure maximum performance.
2. We would like to optimize this model so it can be implemented into embedded system and operating without engineering support.
3. We would like to implement this system into parallel robots such as the delta robot due to its application in the haptic system and its ability to transfer the haptic information between environments. [31, 32, 33].

Bibliography

- [1] GT Allison, RN Marshall, and KP Singer. Emg signal amplitude normalization technique in stretch-shortening cycle movements. *Journal of Electromyography and Kinesiology*, 3(4):236–244, 1993.
- [2] Outlander Anatomy. Jamie’s hand symbol of sacrifice. <http://www.outlanderanatomy.com/wp-content/uploads/2015/05/finger-movements-KLS-edited.jpg>, 2014.
- [3] Dianchun Bai, Chunyu Xia, Junyou Yang, Shouxian Zhang, Yinlai Jiang, and Hiroshi Yokoi. Shoulder joint control method for smart prosthetic arm based on surface emg recognition. In *2016 IEEE International Conference on Information and Automation (ICIA)*, pages 1267–1272. IEEE, 2016.
- [4] NA Bemstein. The problem of interrelation between coordination and localization. *Arch Biol Sci*, 38:1–35, 1935.
- [5] B BioSemi. Biosemi activetwo.[eeg system]. *Amsterdam: BioSemi*, 2011.
- [6] Lori A Bolgla and Timothy L Uhl. Reliability of electromyographic normalization methods for evaluating the hip musculature. *Journal of electromyography and kinesiology*, 17(1):102–111, 2007.
- [7] John Alfred Valentine Butler and Denis Noble. *Progress in biophysics and molecular biology*. Elsevier, 2014.

-
- [8] Carlo J De Luca. The use of surface electromyography in biomechanics. *Journal of applied biomechanics*, 13(2):135–163, 1997.
- [9] George ElKoura. Animating the human hand. 2003.
- [10] Ernest Gardner. Physiology of movable joints. *Physiological Reviews*, 30(2):127–176, 1950.
- [11] Henry Gray. *Gray's anatomy: with original illustrations by Henry Carter*. Arcturus Publishing, 2009.
- [12] Levi J Hargrove, Ann M Simon, Aaron J Young, Robert D Lipschutz, Suzanne B Finucane, Douglas G Smith, and Todd A Kuiken. Robotic leg control with emg decoding in an amputee with nerve transfers. *New England Journal of Medicine*, 369(13):1237–1242, 2013.
- [13] Mohd Fauzi Bin Haris, Pavan Chakraborty, and Rajeeva L. Karandikar. Emg signal based finger movement recognition for prosthetic hand control. *2015 Communication, Control and Intelligent Systems (CCIS)*, pages 194–198, 2015.
- [14] Yoshinori KAWAI and H Harashima. Nikutan. *NTS inc*, 2004.
- [15] Takuhei Kawano and Koichi Koganezawa. A method of discriminating fingers and wrist action from surface emg signals for controlling robotic or prosthetic forearm hand. In *2016 IEEE International Conference on Advanced Intelligent Mechatronics (AIM)*, pages 13–18. IEEE, 2016.
- [16] Toshihiro Kawase, Hiroyuki Kambara, and Yasuharu Koike. A power assist device based on joint equilibrium point estimation from emg signals. *Journal of Robotics and Mechatronics*, 24(1):205–218, 2012.

- [17] Rami N Khushaba and Sarath Kodagoda. Electromyogram (emg) feature reduction using mutual components analysis for multifunction prosthetic fingers control. In *2012 12th International Conference on Control Automation Robotics & Vision (ICARCV)*, pages 1534–1539. IEEE, 2012.
- [18] Loretta M Knutson, Gary L Soderberg, Bryon T Ballantyne, and William R Clarke. A study of various normalization procedures for within day electromyographic data. *Journal of electromyography and kinesiology*, 4(1):47–59, 1994.
- [19] Yasuharu Koike and Mitsuo Kawato. Estimation of dynamic joint torques and trajectory formation from surface electromyography signals using a neural network model. *Biological cybernetics*, 73(4):291–300, 1995.
- [20] C Kothe. Lab streaming layer (lsl). <https://github.com/scn/labstreaminglayer>. Accessed on October, 26:2015, 2014.
- [21] Francesco Lacquaniti and Claudio Maioli. The role of preparation in tuning anticipatory and reflex responses during catching. *Journal of Neuroscience*, 9(1):134–148, 1989.
- [22] SE Mathiassen, J Winkel, and GM Hägg. Normalization of surface emg amplitude from the upper trapezius muscle in ergonomic studies—a review. *Journal of electromyography and kinesiology*, 5(4):197–226, 1995.
- [23] N Ozkaya and M Nordin. Viscoelasticity and biological tissues. *Fundamentals of biomechanics—equilibrium, motion and deformation*. New York: Van Nostrand Reinhold, pages 333–353, 1991.
- [24] Jason A Palmer, Ken Kreutz-Delgado, and Scott Makeig. Amica: An adaptive mixture of independent component analyzers with shared compo-

- nents. *Swartz Center for Computational Neuroscience, University of California San Diego, Tech. Rep*, 2012.
- [25] Adnan Rashid and Osman Hasan. Wearable technologies for hand joints monitoring for rehabilitation: A survey. *Microelectronics Journal*, 88:173–183, 2019.
- [26] Wondae Ryu, Byungkil Han, and Jaehyo Kim. Continuous position control of 1 dof manipulator using emg signals. In *2008 Third International Conference on Convergence and Hybrid Information Technology*, volume 1, pages 870–874. IEEE, 2008.
- [27] Sabyasachi Sahoo, Mallikarjuna Korrapati, Roshan Kumar Hota, and Cheruvu Siva Kumar. Bond graph modelling of a tendon driven prosthetic hand finger for motion and impedance control. In *2016 International Conference on Robotics and Automation for Humanitarian Applications (RAHA)*, pages 1–6. IEEE, 2016.
- [28] Marco Santello and John F Soechting. Force synergies for multifingered grasping. *Experimental brain research*, 133(4):457–467, 2000.
- [29] Laxmi Shaw and Sangeeta Bagha. Online emg signal analysis for diagnosis of neuromuscular diseases by using pca and pnn. *International Journal of Engineering Science and Technology* 0975-5462, 4(10):4453–4459, 2012.
- [30] Duk Shin, Jaehyo Kim, and Yasuharu Koike. A myokinetic arm model for estimating joint torque and stiffness from emg signals during maintained posture. *Journal of neurophysiology*, 2009.
- [31] Sorawit Stapornchaisit and Chowarit Mitsantisuk. Micro-macro bilateral control in delta robot. *International Review of Automatic Control (IREACO)*,

- 8(4), 2015.
doi:10.15866/ireaco.v8i4.6779.
- [32] Sorawit Stapornchaisit, Chowarit Mitsantisuk, Nattapon Chayopitak, and Yasuharu Koike. Bilateral control in delta robot by using jacobian matrix. In *2015 6th International Conference of Information and Communication Technology for Embedded Systems (IC-ICTES)*, pages 1–6. IEEE, 2015.
- [33] Sorawit Stapornchaisit, Chowarit Mitsantisuk, Siwapon Srisonphan, Nattapon Chayopitak, and Yasuharu Koike. Micro-macro bilateral in task space for delta robot by using forward and inverse kinematic. In *TENCON 2014-2014 IEEE Region 10 Conference*, pages 1–6. IEEE, 2014.
- [34] RSL Steeper. bebionic3, 2013.
- [35] KB Veiersted. The reproducibility of test contractions for calibration of electromyographic measurements. *European journal of applied physiology and occupational physiology*, 62(2):91–98, 1991.
- [36] José Manuel Ferrández Vicente, José Ramón Álvarez-Sánchez, Félix De la Paz López, Javier Toledo Moreo, and Hojjat Adeli. *Biomedical Applications Based on Natural and Artificial Computing: International Work-Conference on the Interplay Between Natural and Artificial Computation, IWINAC 2017, Corunna, Spain, June 19-23, 2017, Proceedings*, volume 10338. Springer, 2017.
- [37] Shih-En Wei, Varun Ramakrishna, Takeo Kanade, and Yaser Sheikh. Convolutional pose machines. In *Proceedings of the IEEE Conference on Computer Vision and Pattern Recognition*, pages 4724–4732, 2016.

-
- [38] Jaynie F Yang, DA Winter, et al. Electromyographic amplitude normalization methods: improving their sensitivity as diagnostic tools in gait analysis. *Arch Phys Med Rehabil*, 65(9):517–521, 1984.
- [39] Ting Zhang, Shaowei Fan, Jingdong Zhao, Li Jiang, and Hong Liu. Design and control of a multisensory five-finger prosthetic hand. In *Proceeding of the 11th World Congress on Intelligent Control and Automation*, pages 3327–3332. IEEE, 2014.
- [40] Tong Liu Zhu, Julius Klein, Seraina Anne Dual, Teo Chee Leong, and Etienne Burdet. reachman2: A compact rehabilitation robot to train reaching and manipulation. In *2014 IEEE/RSJ International Conference on Intelligent Robots and Systems*, pages 2107–2113. IEEE, 2014.